UNIVERSITY POLITEHNICA OF BUCHAREST

DOCTORAL SCHOOL OF ELECTRICAL ENGINEERING

PhD THESIS

SUMMARY

Advanced methods for energy transfer analysis in emerging low-inertia power systems

Ing. Radu PLĂMĂNESCU

Scientific Coordinator: prof. dr. ing. Mihaela ALBU

CONTENT

1 Low-inertia power systems

1.1 Emerging power systems. Introduction for inertia issues

The operating paradigm in power systems is changing toward emerging power systems with new and advanced technologies to generate, transmission, and distribution for electric power. These systems often rely on generation from intermittent renewable energy sources interfaced with power electronics. One of the challenges that emerging power systems face is the need to maintain grid stability and reliability despite the variability of renewable energy sources. Consequently, the inertia of the power system decreases as the penetration of RES increases. The reduced inertia in the power system leads to an increase in the rate of change of frequency (rocof) and frequency deviations in a very short time, under power imbalances that substantially affect the frequency stability of the system [149] [153].

In general, inertia is defined as the resistance of a physical object to a change in its state of motion, including changes in its speed and direction. Inertia is a measure of the energy stored in rotating masses within a power system, such as turbines in conventional power plants. [149] This stored energy helps to stabilize the grid by providing a buffer against sudden changes in power demand or supply. However, many renewable energy sources do not have the same level of inertia as traditional power plants, which can make it more difficult to maintain grid stability.

1.2 Active distribution grids. Microgrid concept

In this chapter a short introduction and an analysis of the concept of microgrids is provided, as the microgrids are often characterized as the "building blocks of smart grids", that are perhaps the most promising, novel network structure.[59]. The organization of microgrids is based on the control capabilities over the network operation offered by the increasing penetration of distributed generators including microgenerators, such as microturbines, fuel cells and photovoltaic (PV) arrays, together with storage devices, such as flywheels, energy capacitors and batteries and controllable (flexible) loads (e.g., electric vehicles), at the distribution level. These control capabilities allow distribution networks, mostly interconnected to the upstream distribution network, to also operate when isolated from the main grid, in case of faults or other external disturbances or disasters, thus increasing the quality of supply. Overall, the implementation of control is the key feature that distinguishes microgrids from distribution networks with distributed generation.

Currently, there are multiple definitions for microgrids:

- as a group of interconnected loads and distributed energy resources (DERs) within clearly defined electrical boundaries that acts as a single controllable entity with respect to the grid. The microgrid can connect and disconnect from the grid to enable it to operate in both grid-connected or islanded modes. [21].
- Microgrids can be defined as small, local distribution systems containing generation and load, the operation of which can be separated totally from the main distribution system or connected to it, differing from existing island power systems (such as offshore oil/gas platforms, ships, etc.) in which the connection to and disconnection from the main grid is a regular event [17].
- Microgrids comprise LV distribution systems with distributed energy resources (DER) (microturbines, fuel cells, PV, etc.) together with storage devices (flywheels, energy capacitors and batteries) and flexible loads. Such systems can be operated in a non-

autonomous way, if interconnected to the grid, or in an autonomous way, if disconnected from the main grid [59].

The difference between a microgrid and a passive grid penetrated by micro-sources lies mainly in terms of management and coordination of available resources. A microgrid appears at a large variety of scales: it can be defined at the level of a LV grid, a LV feeder, or a LV house – examples are given in Figure 1-1. In general, the maximum capacity of a microgrid (in terms of peak load demand) is limited to few MW.

In Figure 1-2, the microgrid concept is further clarified by examples that highlight three essential microgrid features: local load, local micro-sources, and intelligent control. In many countries environmental protection is promoted by the provision of carbon credits using renewable energy sources and combined heat and power (CHP) technologies; this should be also added as a microgrids feature. Absence of one or more features would be better described by Distributed Generation interconnection cases or demand side integration cases.

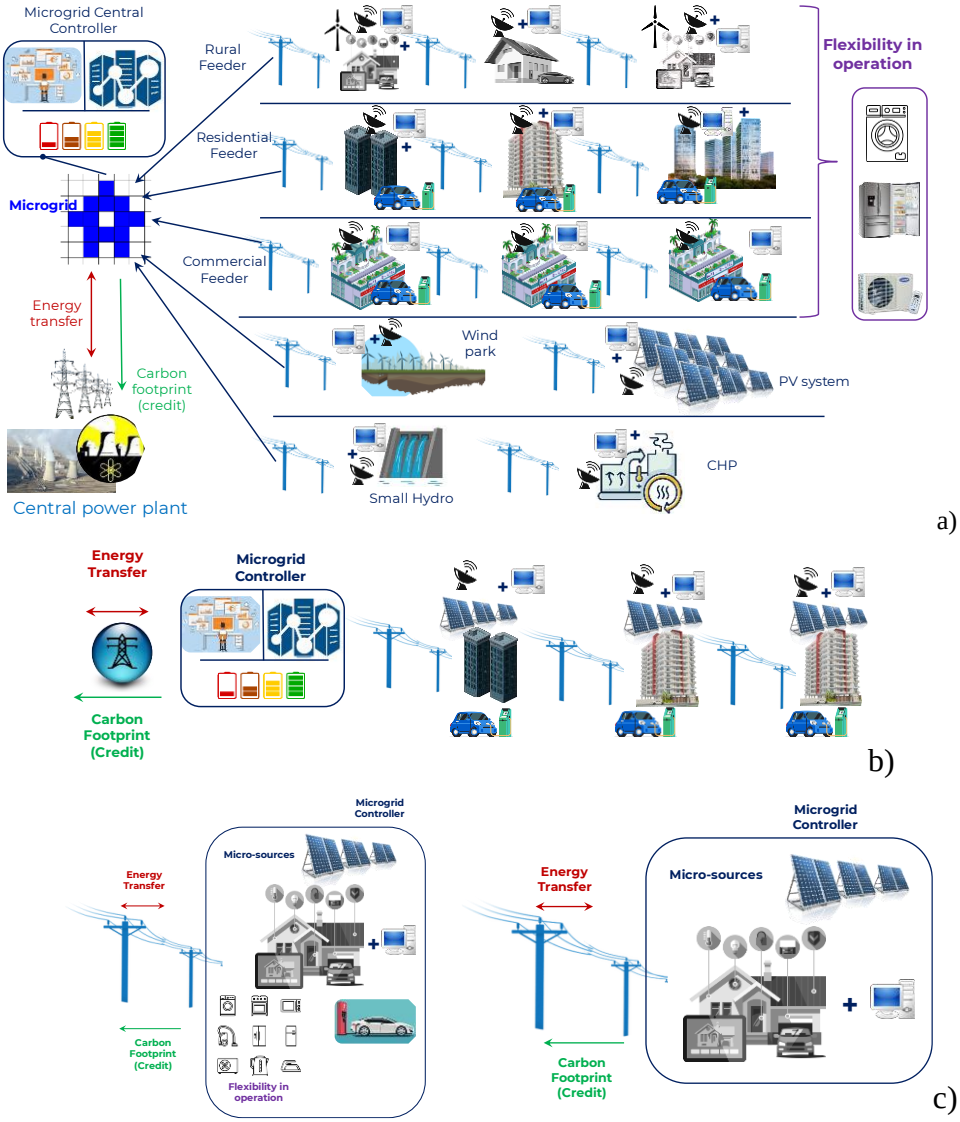

Figure 1-1. Types of microgrids

a) microgrid as a low-voltage grid b) microgrid as a low-voltage feeder c) microgrid as a low voltage house

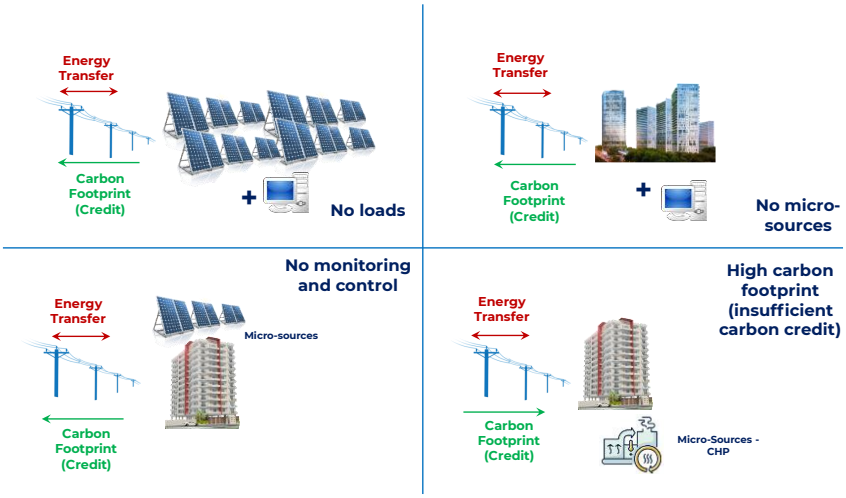

Figure 1-2. Simple examples of what is not a microgrid

1.3 Information aggregation. Definition for energy transfer measurands.

Energy transfer is usually associated with a model characterized by quantities associated with a periodic sinusoidal system. For extracting relevant information for the system under analysis, the aim is to determine the parameters that characterize the energy transfer. In this context, the signals associated with the variables that describe the operation of the system can be described by a minimal set of parameters, the so-called information concentrators. This implies a loss of information by reducing the set of values describing the variation of the measurand during the analysis windows T_m to one or two measured values. Thus, for a periodic signal *x(t)*, the following characteristic parameters of the signal are defined during the measurement windows (average value, rectified average value, RMS value). Moreover, these parameters are subjected to some aggregation algorithms (quadratic averaging or arithmetic) [63] to get reporting rates of measurand compatible with measurement and control systems suitable for inertial power systems (usually 3s).

1.4 Emerging measurement techniques

The approach in this thesis is how to accurately extract information in non-stationary power signals from measurements delivering a measurement result and the associated metrological quality (called from now on, 2M paradigm). To digitally measure a time varying signal, without loss of information, we need to address the relationship between the sampling window of the measurement system and the rate at which the signal is varying [57], [91] together with the model of the signal itself [74]. An additional flagging concept is required to derive a "steady state signal" (called from now on, 3S) based on rapid voltage change monitoring of the IEC 610000-4-30 Standard (3rd edition) [74]. One proposal is for an enhanced definition (called 4M paradigm) by including the steady state flag derived from frequency measurements and with various application-selected thresholds and window durations.

2 Methods for Monitoring Distorted Time-Varying Waveforms

2.1 Non-linear, non-stationary signals for energy transfer

The operation of current distribution grids is impacted by the high variability of the energy transfer. For high efficiency in operation and increased power quality evaluation, awareness over the distorted waveform signals is needed, and thus, a new approximation model for its characteristic quantities (voltages, currents, power). An important issue to be considered is the accuracy of

estimating time-varying distorted voltage and current signals, following fast successive quasi-steady-state operation modes.

2.2 Short Time Fourier Transform (STFT)

Short-Time Fourier Transform It is a method for estimating the spectrum of a signal that changes over time. The meaning of this approach is to divide the signal into several segments of equal length (which may or may not overlap with each other) by using a moving window and then apply the Fourier transform to these segments. The main disadvantage of the STFT may be called the uncertainty principle, which follows from the theoretical limits that the Fourier transform has. When the window size decreases, we know more accurately at what time the signal had this frequency, but at the same time, we know less accurately the value of this frequency. When the window size increases, it does the opposite, we know the frequency value more accurately, but less accurately the time when this frequency was present in the signal. The Fourier Transform using sliding windows is used in high-frequency components identification in variable signals up to 150 kHz, using a method provided in the latest standard IEC 61000-4-7 [78], using implementation specifications from CISPR 16-1-1 [77].

2.3 High-reporting rate measurement equipment

Synchronized measurements are a critical aspect of power system monitoring and control. In a power system, various electrical parameters such as voltage, current, and frequency need to be monitored in real-time to ensure safe and reliable operation. Synchronized measurements are used to measure these parameters with high accuracy and precision, enabling power system operators to quickly identify and resolve any issues that may arise. Phasor Measurement Units (PMUs) are specialized devices used to perform synchronized measurements in power systems. These units measure the voltage and current phasors at specific locations in the power system and transmit this information to a central control system. The PMUs use Global Positioning System (GPS) technology to synchronize their measurements in the power system. PMUs use high-reporting rates for the voltage and current phasors at rates up to 100 frames/second in 50 Hz systems. The measured values are then time-stamped with GPS accuracy (40-50 ns) and transmitted to a central control system for analysis. The central control system can use this data to create a real-time picture of the power system, allowing operators to quickly identify any abnormal conditions and take corrective action.

2.4 Hilbert – Huang Method

The Hilbert–Huang method was firstly introduced in [62] as an innovative tool for the analysis of nonstationary distorted signals to identify time-frequency-magnitude behavior of the mono-components inside the original signal, with later modifications in [115]. The method includes Empirical Mode Decomposition (EMD) enhanced with appropriate chosen masking signals created based on the algorithm of Fast Fourier Transform, enabling this solution to generate truly mono-component intrinsic mode functions (IMFs). Even in this situation, the improved EMD with masking signals will not always guarantee mono-component functions, and a post processing algorithm is proposed after applying the Hilbert Transform over the IMFs obtained. The use of the method and the ability of separating the modes of oscillation within a distorted waveform will be demonstrated as an investigation tool for identification of events in time varying, non-stationary, non-linear waveforms specific for the energy transfer within LV prosumer environment.

2.4.1 Instantaneous frequency

The idea of an "instantaneous frequency" is relevant with the introduction of the Hilbert Transform, which at any time, can compute one value for the frequency that characterizes only one component (and here the introduction of mono-component functions).

2.4.2 Intrinsic mode functions

An intrinsic mode function (IMF) is defined by two principal characteristics: a) its mean is zero and b) the number of local extrema must be equal to or differ by at most 1 from the number of zero crossings within an arbitrary time window. A mono-component signal, by definition, has a unique well-defined and positive instantaneous frequency represented by the derivative of the phase of the signal. A signal, with multiple modes of oscillation existing simultaneously, will not have a meaningful instantaneous frequency. Accordingly, a distorted signal must be decomposed into its constituent mono-component signals before the application of Hilbert transform to calculate the instantaneous frequency.

2.4.3 Empirical Mode Decomposition (EMD)

The essence of the empirical mode decomposition (EMD) is to recognize oscillatory modes existing in time scales defined by the interval between local extrema. The steps comprising the EMD method are as follows:

a1) Identify local maxima and minima of distorted signal, x(t);
a2) Perform cubic spline interpolation between the maxima and the minima to obtain the envelopes $s_M(t)$ and $s_m(t)$;
a3) Compute mean of the envelopes, $m(t) = \frac{s_M(t)+s_m(t)}{2}$;
a4) Extract $c_1(t) = X(t) - m(t)$;
a5) $c_1(t)$ is an IMF if the number of local extrema of is $c_1(t)$ equal to or differs from the number of zero crossings by one, AND the average of $c_1(t)$ reasonably zero. If $c_1(t)$ is not an IMF then repeat steps (a1 – a4) over $c_1(t)$ (instead of x(t)) until the new$c_1(t)$ obtained satisfies the conditions of an IMF.
a6) Compute the residue $r_1(t) = x(t) - c_1(t)$;
a7) If the residue $r_1(t)$ is above a threshold value of error tolerance, then repeat steps a1) – a6) on $r_1(t)$ to obtain the next IMF and a new residue.

2.4.4 Masking signals to separate components

The FFT spectrum of the signal yields its approximate modal content. Masking signals are then required to separate modes of oscillations whose frequencies lie within the same octave, and to accentuate weak higher frequency signals so that they may be sifted out during the EMD.

2.5 A Hybrid Hilbert-Huang Method for Monitoring Distorted Time-Varying Waveforms

The main point highlighted in this section is that Huang's EMD method to determine instantaneous frequency of mono-component signals (mono-component signals called IMFs) is enhanced with appropriate masking signals. This method will be used to study distorted power quality waveforms with multiple modes of oscillation so it must be decomposed into its mono-components before applying the Hilbert transform for instantaneous frequency computation. EMD based on masking signals has its ground base within FFT spectrum. Because when applied to nonstationary and nonlinear distorted signals FFT will approximate signal's modal content, it is only used as a starting point for constructing the masking signals. EMD will be then employed to sift out higher frequency components from the original signal.

The signal $x(t)$, for the analysis window T_a is digitized with appropriate sampling frequency f_s, resulting the discrete signal $x[p]$, with limits of error e_{lim} depending on the instrumentation chain (usually 2%, for normal operating condition). For the type of low voltage prosumer equipment today f_s should be bigger than 10 kHz. In this work it has used a sampling frequency $f_s = 20\ kHz$ and an analysis window of $T_a = 1s$. The steps are as follows:

1. $x[p]$ (corresponding to $x(t)$ during T_a) is decomposed into its modes of oscillation with the help of the Empirical Mode Decomposition (EMD) proposed by Huang in [62] but enhanced with masking signals (obtained by applying a Digital Fourier Transform on the original signal $x[p]$).
2. Masking signals are created using the algorithm proposed in [13] and, because the process is based on resulting frequency [global] spectrum, the novelty/improvement here is related to the adequate selection of the components (amplitudes and frequencies) of interest by setting a threshold, discriminating useful information from noise.
3. By deploying Empirical Mode Decomposition (EMD) on the digitized signal, mono-component functions called intrinsic mode functions (IMFs) will be obtained. Each of the IMFs, for a random time window, has its mean equal to zero and the number of local extrema equal to or different by at most 1 from the number of zero crossings.
4. After obtaining IMF components, Hilbert Transform is applied to compute amplitudes and the corresponding (instantaneous) frequencies in the individual intrinsic mode functions (IMF) components. By such, intrinsic mode function (IMF) decomposition emulates a generalized Fourier expansion with improved efficiency and applicability for non-stationary data (characterized by variable amplitudes and frequencies).
5. In some cases, when the improved EMD with masking signals does not deliver mono-component IMFs signals, further demodulation is advised after Hilbert Transform. By performing the Hilbert Transform it can be observed a resultant modulation.

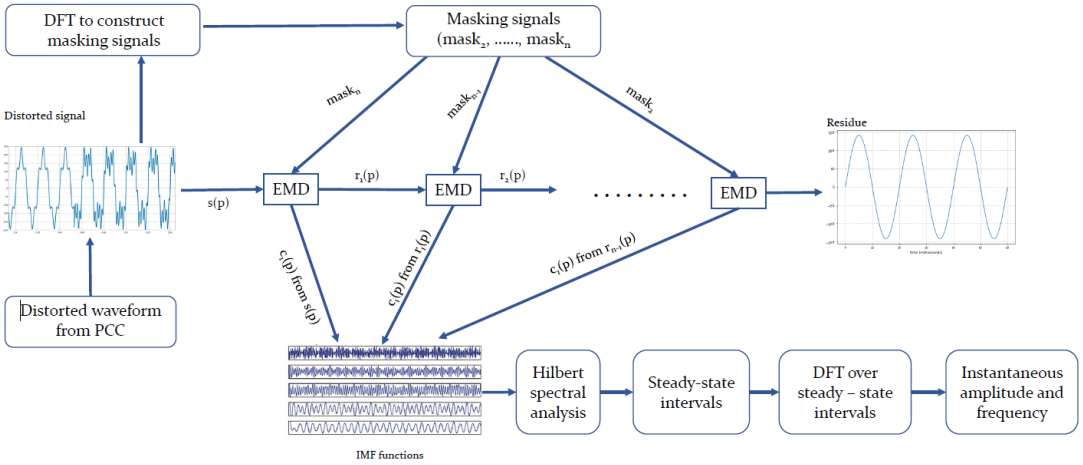

Figure 2-1. Framework for decomposing distorted signal into high-frequency components using Hilbert–Huang method.

6. A post processing method is proposed since each intrinsic mode function (IMF) approximates the modes of oscillation within the signal. The novelty of the method presented in this paper is for identification of quasi steady – state time intervals based on the instantaneous frequency computed using Hilbert Transform. By obtaining and detecting the time intervals where the signal has a constant variation, basic DFT is computed to obtain the true amplitudes and frequencies of the inner components of the original signal.

The approach of the method is a continuation of the one proposed in [150] with the aim of improving its performances and expanding the area of applications involving distorted waveforms analysis and it is presented in Figure 2-1.

2.5.1 Versatile Discrete Fourier Transform and Masking Signals to Improve the empirical mode decomposition

The methodology and the analytical approach used to construct such masking signals is now improved with the innovative versatile DFT essential for computing the parameters of the masking signals. The ground base of creating such signals is the DFT spectrum that will only be used as a starting point of the method, as the Fourier Transform approximates non-stationary, non-linear distorted waveforms modal content. The original current signal $i(t)$ subjected to the investigation window T_w is digitized with proper sampling frequency f_s resulting the discrete signal $i[p]$. Afterwards, the estimated frequencies and associated amplitudes will be adequately selected out of the resulting frequency spectrums, and masking signals will be created based on the Discrete Fourier Transform.

2.5.2 Enhanced empirical mode decomposition with Masking Signals

Empirical Mode Decomposition (EMD) method is used for time-varying, nonstationary, nonlinear waveforms to split them into multiple intrinsic mode functions (IMFs) that possess the well-behaved Hilbert Transform conditions.

2.5.3 Post—Processing Method

For non-stationary, nonlinear, distorted waveforms, the approach of this thesis considers a new algorithm as per the post processing part, applied over the results of the Hilbert Transform. The objective is to allow identification and segregation of quasi-steady-state subintervals within the total signal analysis window. The final detection of such time intervals will be conducted based on an updated version of the Rapid Voltage Changes (RVC) algorithm as defined in IEC 61000-4-30 [63] and modified to fit into our hybrid algorithm. The updated version of the algorithm will be called Quasi-Steady-State Identification (QSSI). The final step will consist of identification of frequencies and amplitudes of the original digitized signal's inner components, to be calculated based on a DFT algorithm executed over the identified quasi stationary intervals.

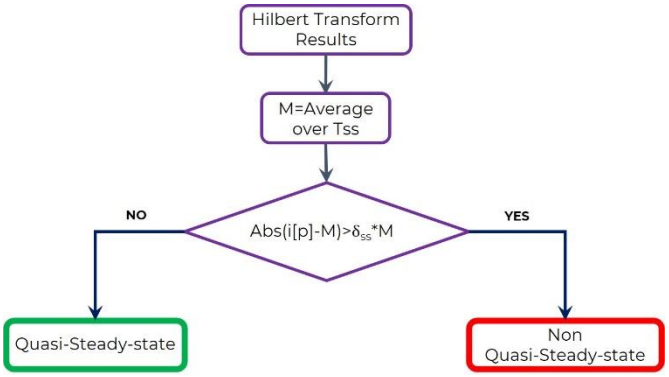

Figure 2-2. Quasi-Steady-State Identification (QSSI) algorithm used for the hybrid Hilbert-Huang

2.5.4 The Ability of the Method to Separate Components

A synthetic digitized current signal is created to validate the method. A distorted signal emulating the parameters of the current in a common-coupling point for an energy community is constructed with a sampling frequency of 51.2 kHz, with a fundamental frequency of 50 Hz and multiple time-varying components as described in Table 2-1. For this simulation, as can be seen in the table, the

components do not appear on the whole-time window (T_w), but on some intervals only, their amplitudes being expressed in percentages of the RMS value of the original signal.

Table 2-1. Components of the original signal under investigation.

Time [s]	**Component Amplitude (% of RMS of Signal)**				
	150 Hz	**250 Hz**	**350 Hz**	**430 Hz**	**450 Hz**
0–0.253	23%	9%	19%	0%	0%
0.253–0.450	14%	0%	5%	0%	5%
0.450–1	0%	15%	0%	15%	0%

The signal as described in the table above is plotted on Figure 2-3a together with its DFT spectrum (Figure 2-3b) of the components delivered by the Fourier analysis. DFT spectrum is the first step evolved in the hybrid Hilbert-Huang.

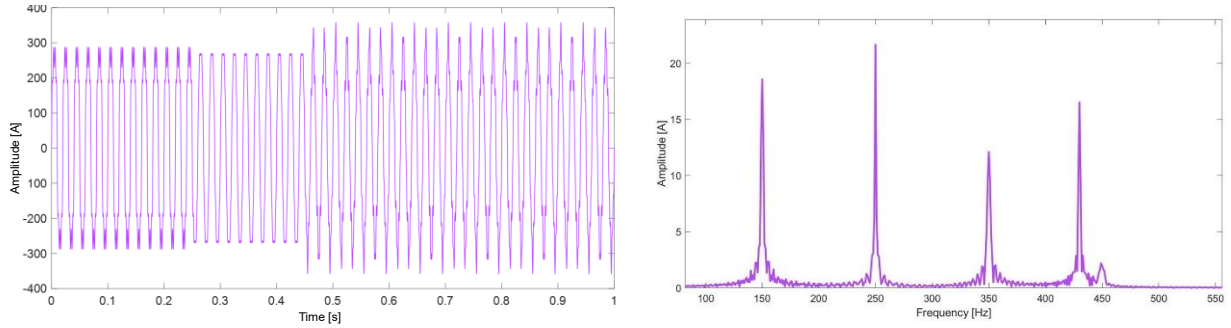

a) b)

Figure 2-3. (a) Original digitized signal described in Table 1, (b) Discrete Fourier Transform (DFT) spectrum of the original signal-range 100 Hz to 550 Hz.

Based on the frequency information obtained from the DFT spectrum, masking signals were created to improve EMD tool and to properly extract four mono-component IMFs. Over each IMF, Hilbert Transform was applied, then a moving average filtered the results, and finally, with the help of the innovative post-processing method described in Section 2.5.3 three quasi-steady-state intervals were identified. One mention must be done because some parts were discarded based on the transitional aspects of the original signal, from one interval to the adjacent one and because of the artefacts at the end of the time window. Having obtained those time intervals, Hanning windows were applied over each interval, obtaining the following signals, as can be seen in Figure 2-4.

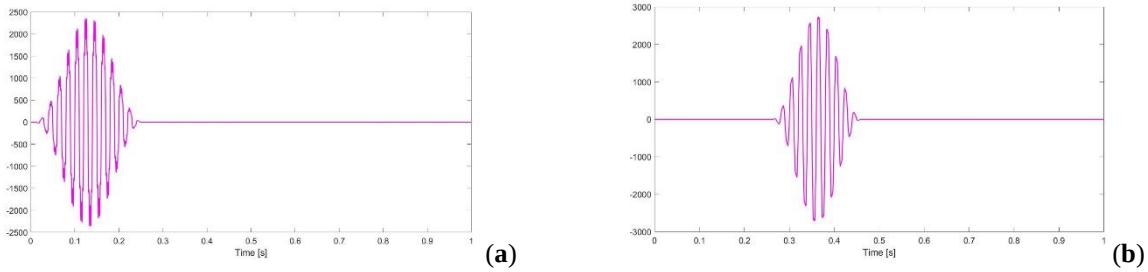

(**a**) (**b**)

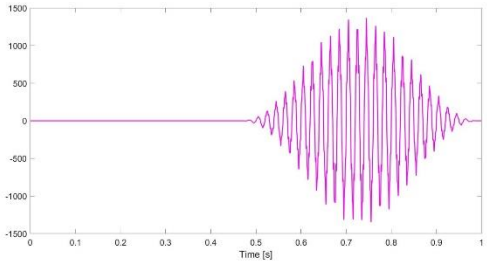

(**c**)

Figure 2-4. (a) First quasi-steady-state interval enhanced with a Hanning window, (b) second interval enhanced with a Hanning window, (c) last interval enhanced with a Hanning window

With the objective of identifying and separate the modes of oscillation inside the original distorted signal, with the quasi-steady-state intervals computed, we can now apply DFT over each of these time intervals and calculate the instantaneous frequencies and the amplitude of the inner components of the non-stationary, non-linear original signal. The final frequencies and the corresponding amplitudes are shown in Figure 2-5, as the method successfully traced the mono-components, identified the time intervals, and the DFT applied once again on quasi-steady-state intervals.

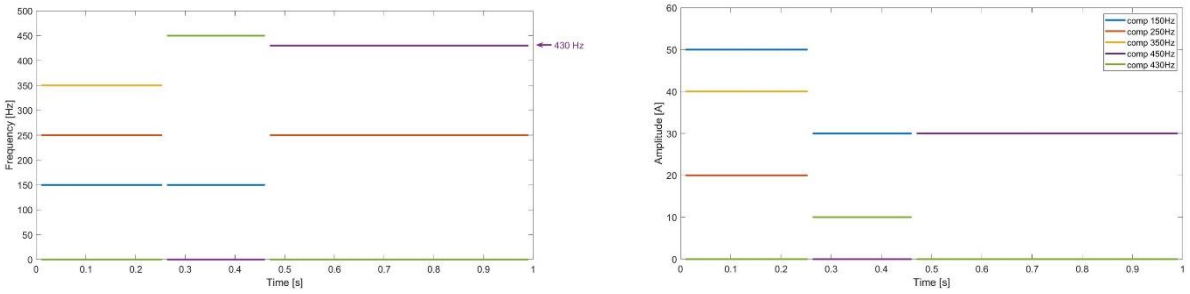

(**a**) (**b**)

Figure 2-5. **(a)** Instantaneous frequencies and (b) amplitudes, of the mono-components extracted using the hybrid Hilbert-Huang method, of the synthetic signal described in. Table 2-1

2.5.5 Demonstration

A real distorted time-varying current waveform specific for a microwave oven is used and the measurement data were provided by an ELSPEC Power Quality analyzer [37]. The current waveform digitized at a sampling rate of 1024 samples per cycle, or 51.2 kHz, was studied over a $T_w = 7s$ time-window. The time window was appropriately chosen to capture the very particular cycle-based way of operating of a microwave oven. The rated input power of the under-investigation oven is 1200 W. As it will be shown in Figure 2-6, the current varies from approximate 8 A (peak-to-peak value) to 0.3 A and then back again to 8 A with a 1 s transition when the current reaches 4 A, peak-to-peak value. Significant 150 Hz and 250 Hz time varying components are expected to be identified within the time window, but also 100 Hz, 200 Hz, and 350 Hz. The original signal and the associated DFT spectrum are depicted in Figure 2-6.

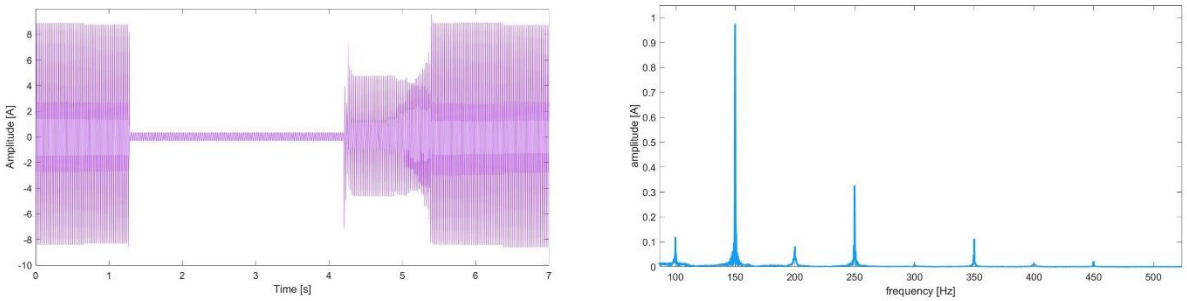

(**a**) (**b**)

Figure 2-6. (a) Original digitized current signal of a microwave oven, (b) DFT spectrum of the original signal-range 100 Hz to 500 Hz.

The main frequencies, other than the fundamental one, are, as can be seen above, 100 Hz, 250 Hz, 200 Hz, 250 Hz, and the 350 Hz. It is to be noted that the DFT spectrum is spread over a range of frequencies thus causing the amplitude information to be subjected to a resultant uncertainty. The first step in applying the enhanced EMD was to construct masking signals, as visually described in Figure 2-1. Based on the versatile DFT spectrum, four modes of oscillation were identified within the signal at 100 Hz, 150 Hz, 250 Hz, and 350 Hz. For those components, appropriate masking signals were constructed with 150 Hz, 250 Hz, 400 Hz, and 600 Hz. IMF 4 will be considered negligible in amplitude, and it will be discarded from the analysis, and the Hilbert Transform will be applied over the remaining IMFs.

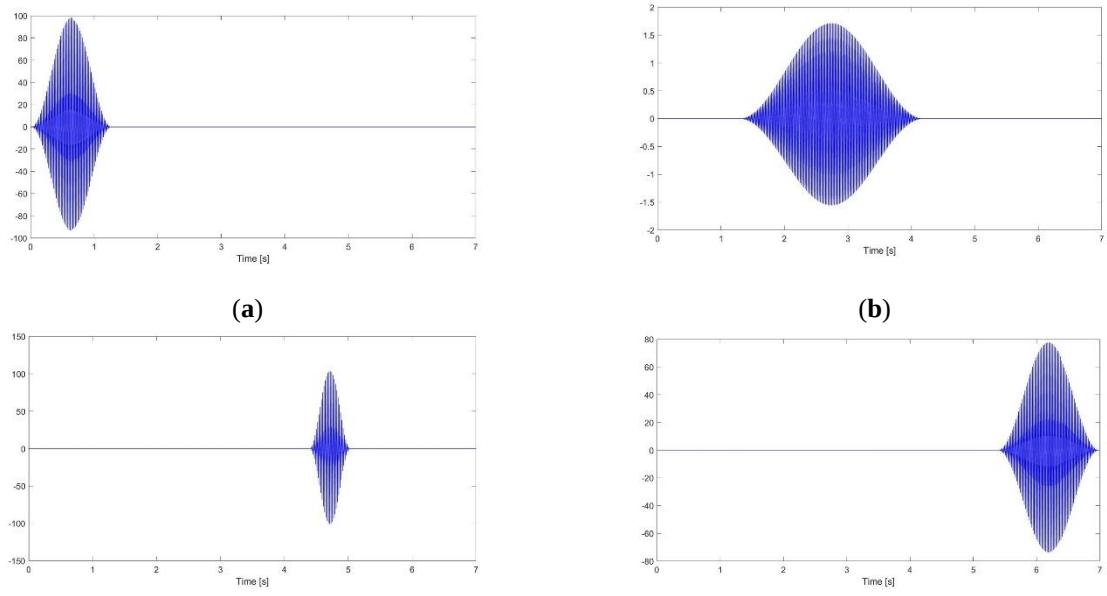

(**a**) (**b**)

(**c**) (**d**)

Figure 2-7. Quasi-steady-state intervals enhanced with Hanning windows: (a) First interval, (b) second interval, (c) third interval subjected to EMD for a second time, (d) fourth interval.

The novelty underlined within this paper in terms of quasi-steady-state time intervals identification is the next step in the intended application of the hybrid method. QSSI proves its practicality when it comes to non-stationary non-linear distorted power signals for which further investigation is required. Detection of steady-state time intervals within a distorted power waveform together with the associated frequency content is opening a wide range of potential applications such as load and generation signature profiling, power system event diagnosis, distribution transfer function

estimation, etc. After filtering the results of Hilbert Transform, the algorithm for identification of quasi-steady-state intervals was enabled and four time-intervals were detected. Out of those, only three of them could be called quasi-steady state, with the remaining one to be subjected to further EMD analysis. The resulting intervals enhanced with the Hanning window are shown below in Figure 2-7. The final post-processing part applied over this time interval shows a quasi-steady-state identification only for half of the total interval; for the rest we can conclude there are only transitional components, and thus discarded those artifacts. Along with the example for a synthetic signal, the edges of the observation time window were discarded, as well as the transitions between the identified time intervals. The instantaneous amplitudes and frequencies after applying post-processing algorithm and then DFT over the quasi-steady-state intervals, are shown in Figure 2-8. DFT was applied over the entire time window (T_w) under investigation but enhanced with Hanning function resulting in a 1 Hz frequency resolution.

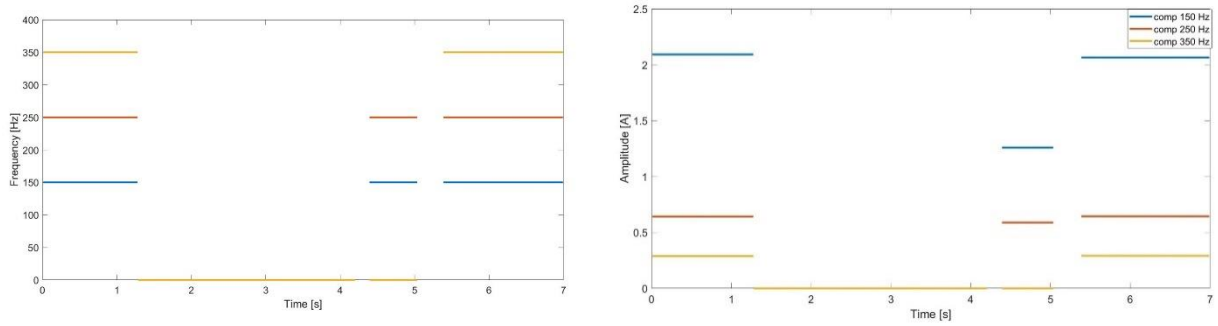

(**a**) (**b**)

Figure 2-8. (a) Instantaneous frequencies and (b) amplitudes, of the mono-components extracted using the hybrid Hilbert-Huang method, of the microwave oven current described in Figure 2-6

To validate the proposed hybrid algorithm, a power analyzer was used as a reference in terms of results computation, using time-varying frequency content as an input signal. As per [37], this equipment performs DFT every 1 cycle and can provide up to 512 harmonics of the 50Hz fundamental; it also performs DFT over a 10-cycle window, providing the frequency components with 5 Hz resolution, but also lacks in identification of abnormal components such as the mode of oscillation with 430 Hz (as per the synthetic signal above) or 494 Hz.

3 High reporting rate smart metering data for enhanced grid monitoring and services for energy communities

A new generation of smart meters need to comply with three main demands: lower cost, high quality information (for example, using reporting rates like 1 frame per second or higher) and ensuring privacy or cyber security of data. An example of smart meter answering to those requirements is the Unbundled Smart Meter concept [120], developed around two components: Smart Metrology Meter (SMM) which is the metrological part and covers all the hard real-time functions with fixed (frozen) functionality and the Smart Meter eXtension (SMX), which has a high grade of flexibility and brings new functionalities to the SMM for supporting the future evolution of smart grid and energy services.

3.1 Information loss using aggregated values

The main ideas and features of the next generation smart meters used in this work are identified as to have a closer look of the dynamics of the LV nodes and to use appropriate statistical metrics within the meter itself. [108].

For the measurement campaign, it has been made use of two types of USMs. The SLAM meter [120] is an advanced high-reporting rate (0.5 frames/s) multi-function digital single-phase smart meter Class B in active energy and Class 2 in reactive energy, which complies with European legislation related to energy meters (MID) EN 50470-1 and EN 50470-3. The other type of USM is a high reporting rate (1 frame per second) measurement equipment consisting of a SMX connected to a commercial smart meter LandisGyr [97] that is a three-phase energy meter (IEC 62053-21 class 1) and reactive energy (IEC 62053-23 class 2).

3.2 Trial site description

The pilot site chosen for demonstrating and implementing a strong and reliable smart metering infrastructure was the student campus (Regie) of the University POLITEHNICA of Bucharest (UPB). Following the office type nonlinear loads, there is a potential of non-symmetric loading conditions on each phase which might give rise to several PQ issues, or even interruption in power supply. A thorough analysis of the network needs synchronized information (from all buildings) with high time granularity. For the actual implementation of the site trial within the campus, for 5 of the total 27 student buildings smart meters were installed insuring a coverage of almost 20% of the entire power profile. An overall simplified topology of the pilot site can be seen in the picture below, in Figure 3-1.

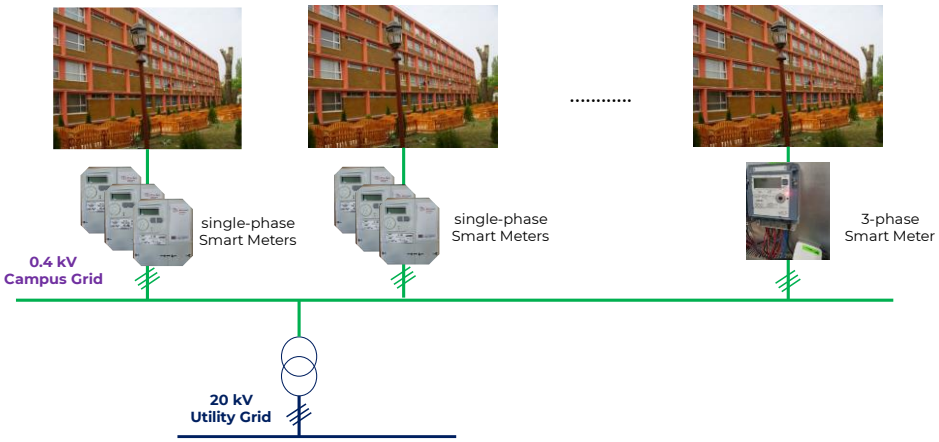

Figure 3-1. Simplified grid topology of the campus with smart meter installation [49].

The metering infrastructure includes 39 one-phase SLAMs (Smart Low-Cost Advance Meter) and 12 three-phase USMs (Unbundled Smart Meter). These measurement systems are covering the energy supply for 1840 students. The information used in this paper was extracted from energy meters installed in a student building with 150 rooms and 300. The use was for single-phase energy meters installed on each floor.

3.3 Methodology for information loss evaluation

The averaged power profiles were computed for 1 min aggregation, 15 min aggregation and 1h aggregation. It has been used a simple averaging algorithm of the 2s (1s) resolution information received from the field smart meters. A visual representation of the process for information aggregation can be seen in Figure 3-2.

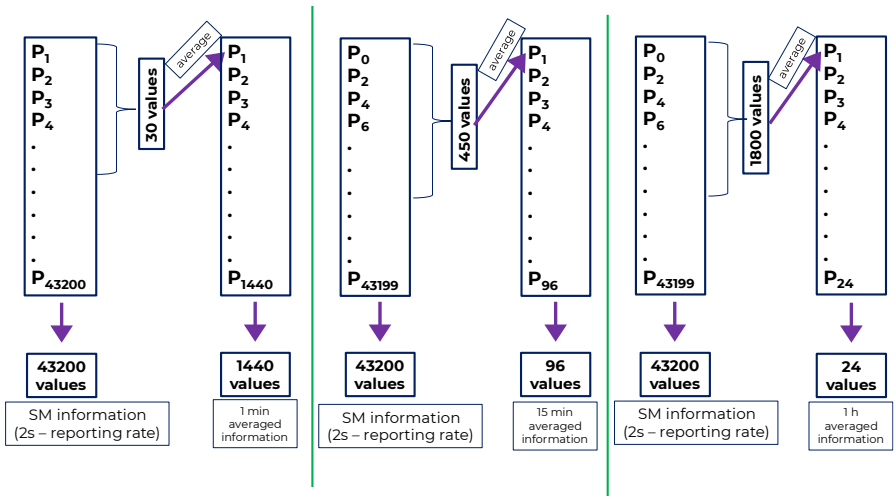

Figure 3-2. Information aggregation for 0.5 frames/s reporting rate smart meters

Let us name each reported measurement for active power by the smart meter (with 2s resolution) where x is ranging from 1 to 43200. Thus, active power reported in one day consists in 43200 values (ranging from P_1 to P_{43200}).

As such, for 1 min aggregation, the information is computed by arithmetic average of sets of 30 values (number of reported measurements in 1 min with 2s resolution). A generalization of the averaging process for 1 min aggregation is given in equation (3.1)

$$\overline{P_i^{1min}}[t] = \frac{P_{i\cdot 30+1} + P_{i\cdot 30+2} + \cdots + P_{i\cdot 30+30}}{30} \tag{3.1}$$

, where i ranges from 0 to 1439.

For 15 min aggregation, the information is computed by arithmetic average of sets of 450 values (number of reported measurements in 15 min with 2s resolution). A generalization of the averaging process for 15 min aggregation is given in equation (3.2)

$$\overline{P_i^{15min}}[t] = \frac{P_{i\cdot 450+1} + P_{i\cdot 450+2} + \cdots + P_{i\cdot 450+450}}{450} \tag{3.2}$$

, where i ranges from 0 to 95.

For 1h aggregation, the information is computed by arithmetic average of sets of 1800 values (number of reported measurements in 1h with 2s resolution). A generalization of the averaging process for 1h aggregation is given in equation (3.3)

$$\overline{P_i^{60min}}[t] = \frac{P_{i\cdot 1800+1} + P_{i\cdot 1800+2} + \cdots + P_{i\cdot 1800+1800}}{1800} \tag{3.3}$$

, where i ranges from 0 to 23.

The information loss algorithm was computed using the standard deviation formula between 2s information and mediated information for each of the studied cases.

$$std\_agg_{interval} = \sqrt{\frac{\sum(P_x - \overline{P_i})}{N}} \tag{3.4}$$

, where P_x is the reported active power (2s resolution) and $\overline{P_i}$ is the averaged value (depending on the case, 1min, 15min, 1h) corresponding to the interval where P_x belongs. *Interval* indicates that the standard deviation is computed for all the studied cases (1min, 15min and 1h).

The result was then divided by the 24h mean of the respective day (as per equation (3.5) resulting the final value of the information loss (as per equation (3.6))

$$P_{mean}^{1\ day} = \frac{\sum_0^{N-1} P_{2\cdot i}}{N} \tag{3.5}$$

, where N is the total number of reporting measurements in one day (in our case 43200).

$$info\_loss_{interval} = \frac{std\_agg_{interval}}{P_{mean}^{1\ day}} \tag{3.6}$$

, where *Interval* indicates that the variable is computed for all the studied cases (1min, 15min and 1h).

The information loss is the final number with significant importance for our paper and it is highlighted the figures and in the comments of the manuscript.

3.4 Experimental results

To highlight the information loss when using averaged power profiles instead of those obtained from smart meters with 0.5 or 1 frames/s reporting rate, in case of daily load power profiles of student campus buildings, several scenarios were studied given the three-phase connections. The main aspects considered when studying the power profiles were temporal features (for days of the regular university semesters, type of days of normal behavior (depending on weekday or weekend day). climate consideration (for winter and summer days with a lot of heating and cooling systems), electrical features (given the three-phase system of a student building, 1-phase studies, and three-phase studies). Following subsections will highlight only some of the cases under analysis, only some examples of the power profiles will be plotted and presented.

3.4.1 Scenario for a single-phase power profile for one of the floors of the student building

Measurements results for 24h operation during winter and summer for both weekdays and weekend days are presented. The information is for 30 rooms and 60 students. It can be observed the classical power profile with high demand during the evenings and mornings and low demand for afternoons and nights.

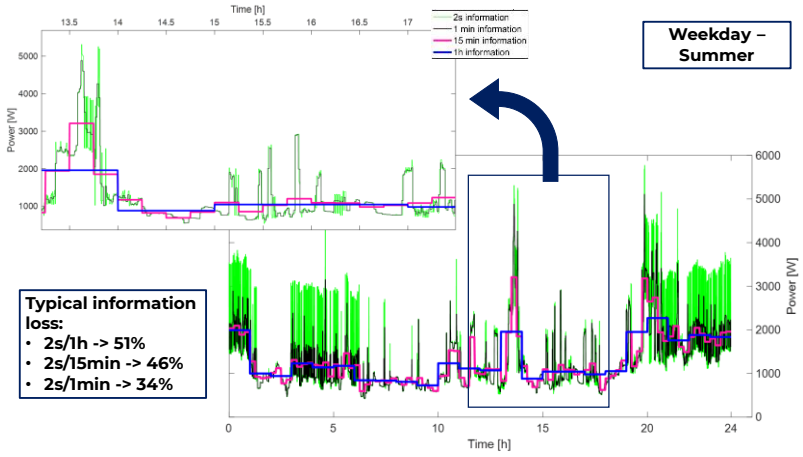

Figure 3-3. Power profile (singe-phase) for one floor of the building with 30 rooms and 60 students– weekday in the summer

3.4.2 Scenario for a single-phase power profile for the entire student building (spatial aggregation)

Measurements results for 24h operation during winter for 150 rooms and 300 students (single phase)

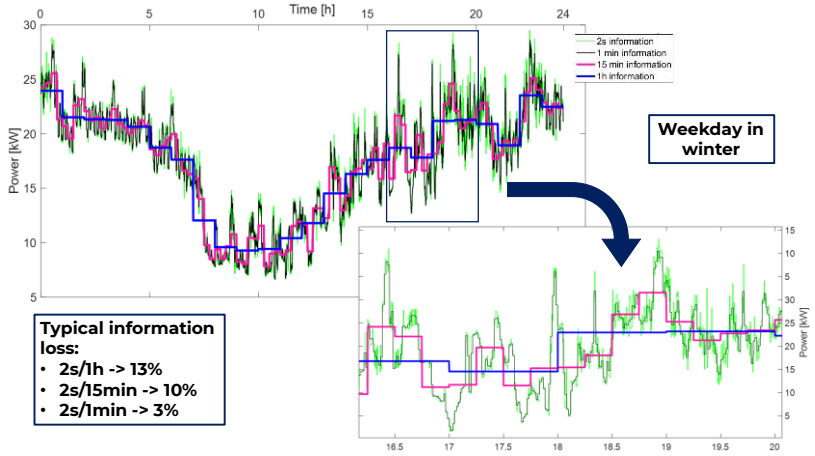

Figure 3-4.Power profile (singe-phase) for the building with 150 rooms and 300 students– weekday in the winter

The power profile depicted in the following figures was computed by summing up the active power information extracted from each meter on phase 1 (as suggested in equation (3.7)).

$$P_1[t] = P_1^{et\,0}[t] + P_1^{et\,1}[t] + P_1^{et\,2}[t] + P_1^{et\,3}[t] + P_1^{et\,4}[t] \quad (3.7)$$

3.4.3 Scenario for the three-phase power profile for the entire student building

Measurements results for 24h operation during winter in the weekend for 150 rooms and 300 students (three-phase).

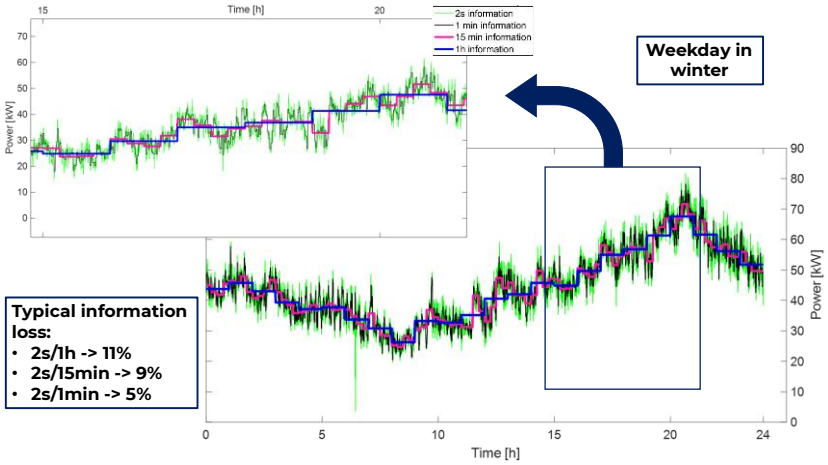

Figure 3-5. Power Profile (three-phase) for the building with 150 rooms and 300 students– weekend in the winter

The power profile depicted in the following figures was computed using the equation (3.11), by summing up the active power information extracted from each meter on each phase (using equations (3.8) – (3.10)).

$$P_1[t] = P_1^{et\,0}[t] + P_1^{et\,1}[t] + P_1^{et\,2}[t] + P_1^{et\,3}[t] + P_1^{et\,4}[t] \quad (3.8)$$

$$P_2[t] = P_2^{et\,0}[t] + P_2^{et\,1}[t] + P_2^{et\,2}[t] + P_2^{et\,3}[t] + P_2^{et\,4}[t] \quad (3.9)$$

$$P_3[t] = P_3^{et\,0}[t] + P_3^{et\,1}[t] + P_3^{et\,2}[t] + P_3^{et\,3}[t] + P_3^{et\,4}[t] \quad (3.10)$$

$$P_t[t] = P_1[t] + P_2[t] + P_3[t] \quad (3.11)$$

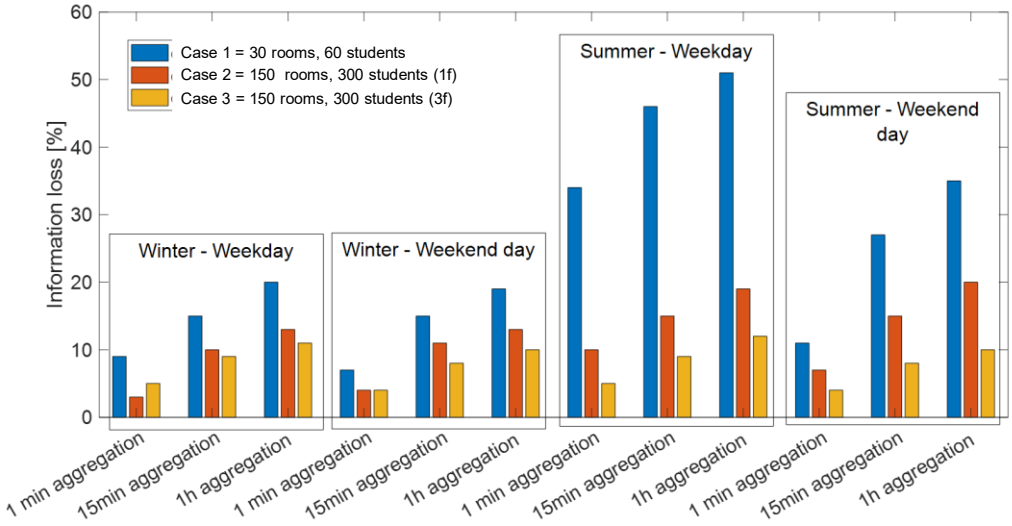

Figure 3-6. Summary of information loss for all the studied cases.

3.5 Comments on the information loss for power profiles

In Figure 3-6 above, it can be observed the information loss variation for all the cases studied and described in this paper. It can be summarized here all the case based on the data plotted below, studied for winter and summer, weekday, and weekend day.

Those findings are in line with the assumption that spatial aggregation (customers supplied on each floor) is acting favorably in what concerns the levelized power profile (temporal aggregation) and therefore the need of high reporting rate (1 frame/s) is limited to individual customers.

3.6 High reporting rate smart metering data for enhanced grid monitoring and services for energy communities

3.6.1 Context and methodology

This section proposes a framework for knowledge extraction from high reporting-rate smart metering data. The process takes place at smart meter level and with low computation and communication costs and preserving user privacy, with the scope to increase the accuracy of the monitoring tools for distribution power grids. The methodology makes use of statistical metrics able to capture system dynamics relevant for network diagnosis. For most of the applications for low-voltage network services, reporting rates of one hour or half an hour were usually considered as sufficient, because the amount of RES penetration was relatively low. However, increased spatial granularity of the energy exchange in modern distribution networks accommodating large number of prosumers and dispersed generation requires monitoring of the power transfer instead of the energy balancing [92]. The focus is on using high resolution datasets of real-time measurements such as voltage, current and active power (in rms values), to allow defining new indices for assessing the network capacity and its voltage smoothness from the usual utility reporting rates, which currently are at 15-, 30- or 60-minutes.

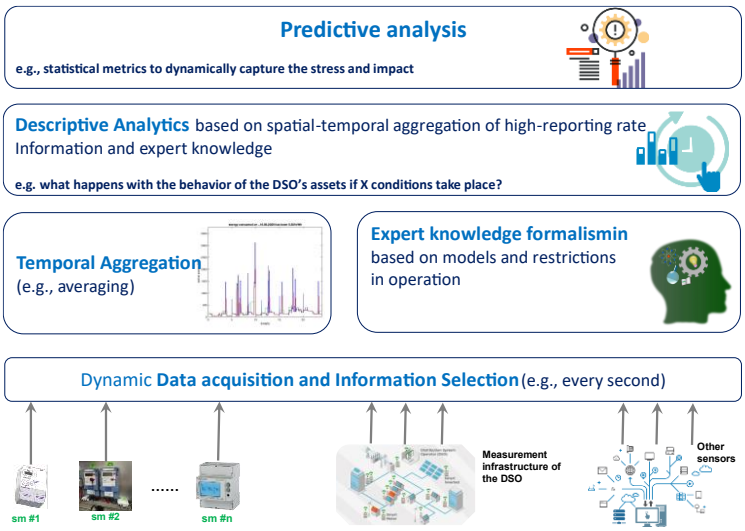

Figure 3-7. Framework for knowledge extraction from high resolution dynamical smart-meter data.

The methodology assumes as baseline scenario the ideal case when the network operator has access to 1-second data. For comparison purposes, three use-cases are investigated against this baseline scenario. Two of them refer to the current utility practices, when only temporal-aggregated energy data is transmitted either every 1-hour (case A) or down to every 15-minutes (case B). The third use-case deals with the 1-minute reporting rates (case C). To critically assess this problem, a general knowledge extraction framework is proposed in Figure 3-7. The framework has four layers: (L1) data collection layer which includes the LV level metering sources and an optional data collection and synchronization process for information coming from external sources; (L2) temporal aggregation layer for the local data integrating an expert knowledge formalism; (L3) descriptive analytics layer for both streams of information from the previous two layers; and (L4) prescriptive analytics and knowledge extraction layer.

Our analysis investigates the behavior of the network following a full diurnal cycle (e.g., total number of Q4 samplings being T = 86400 = 3600s×24h)

a statistical metric of their frequency of occurrence and severity within the aggregation window is a useful information, similar to the assessment of voltage dips. Such metric is the cumulative distribution function (cdf). In the case of active power, ensuring a reliable and safe grid operation requires that their values in the defined (standardized) time intervals lie within limits in more than 95% of their occurrences. Because some of these bounds are not symmetric relative to the standardized (e.g., nominal or optimal) operating values we first apply a decomposition of the signal (1-second measurements) to count the positive (upwards) and negative (downwards) exceeds against the to-be-reported smart meter aggregated value. The proposed aggregation process is able to capture the asymmetrical variations of the signal. This is important because in some diagnostic applications the upward limits might be different than the downwards limits. This approach defers from the power quality aggregation procedure using the quadratic mean (insensitive to the asymmetrical variation of the signal. An example of this decomposition is presented in Figure 3-8 for 15min and 1h aggregation.

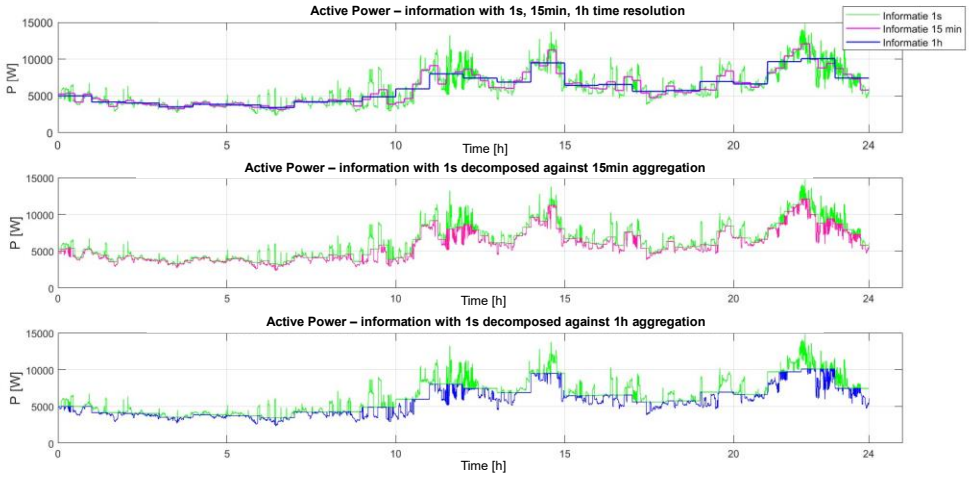

Figure 3-8. Decomposition of active power, P at 1-second, for the student building power profile against 15-minutes and 60-minutes time windows.

Then, on each aggregation window, a recursive discrete calculation is made for the percentiles of interest in the case of measured active power. An illustrative example is provided in Figure 3-9. Several percentiles bounds, also called confidence bounds, per type of aggregation time window could be created for the rules guiding the prescriptive analytics in Layer L4

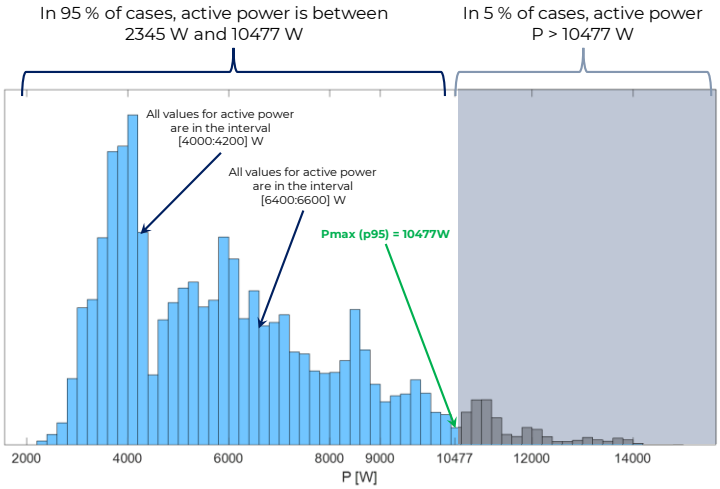

Figure 3-9. Illustrative calculation of the 95-percentile for active power (aggregation time window wa=15-minutes, and Pmax(p95) = 10477W

3.7 Use-cases and results evaluation

To prove the proposed approach the active power information associated with the student building described above was used. The analysis was done for use-cases associated with power profiles based on the spatial and temporal aggregation (for 150 rooms and 300 students for summer/winter, weekday, and weekend scenarios). Below, only one case is presented.

a) **Case 1**, weekday in summer. (Figure 3-10)

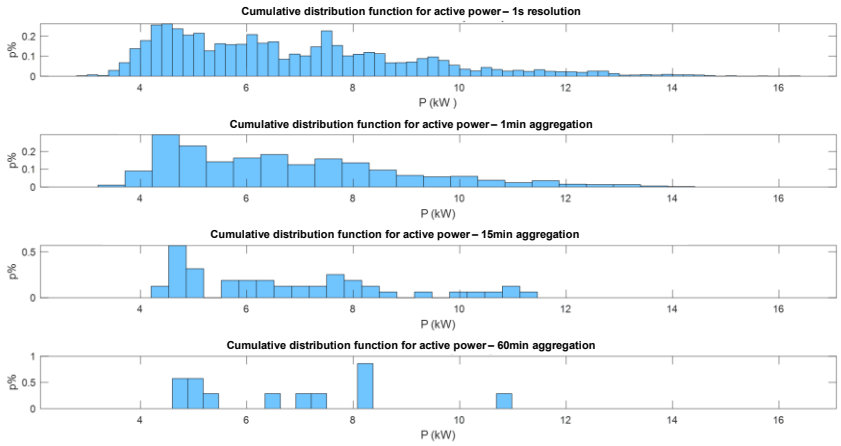

Figure 3-10. Cumulative distribution function for active power using measurement information with 1s, 1min, 15min, 60 min time resolution – for a weekday in summer

Temporal Resolution	p95 [kW]	p99 [kW]	maxP [kW]	1-p99 relative to 1s information	1-maxP relative to 1s information
Case 1, weekday in summer					
1 second	10,477	12,140	14,856	0%	0%
1 minute	10,319	12,008	13,984	1,09%	5,87%
15 minutes	9,985	12,077	12,077	0,52%	18,71%
60 minutes	9,675	10,071	10,071	17,04%	32,21%
Case 2, weekend day in summer					
1 second	11,342	13,427	16,232	0%	0%
1 minute	11,112	13,137	14,902	2,16%	8,19%
15 minutes	10,634	12,219	12,219	8,99	24,72
60 minutes	10,737	10,980	10,980	18,22%	32,35%
Case 3, weekday in winter					
1 second	24,727	27,143	29,523	0%	0%
1 minute	24,633	27,046	28,607	0,35%	3,1%
15 minutes	24,24	25,57	25,57	5,81%	13,4%
60 minutes	23,541	23,953	23,953	11,75%	18,87%
Case 4, weekend day in winter					
1 second	25,442	27,761	30,095	0%	0%
1 minute	25,349	27,498	29,39	0,95%	2,34%
15 minutes	24,731	26,412	26,412	4,86%	12,24%
60 minutes	24,239	25,072	25,072	9,69%	16,69%

Traditionally recorded 15- and 60-minutes discretized power profiles give significantly lower p95 and p99 values because they do not capture the dynamics characterized by high spikes, thus hindering quality of supply issues as well as abnormal loading conditions.

4 Exploiting flexibility under regulatory constraints in a microgrid with highly variable power profiles

4.1 Context

The concept of self-RES consumption communities (SCC) also known as renewable energy communities (REC) is an emerging trend in Europe aiming to fulfil the targets of the most recent "Clean Energy for all Europeans" package. The goal of a self-RES consumption community (SCC), as it is defined in [44], is to increase the volume of locally RES-based generation to an extent higher than the one enabled by the power profile of each prosumer in the community. However, its real potential is rather underestimated, and the new models required by the real time operation in low inertia grids are to be proposed.

4.2 Problem definition

The self-RES consumption community (SCC) under analysis is composed by 2 UniRCons interconnected with a DC link, acting as a low-voltage hybrid (AC+DC) microgrid (MG). The hybrid MG is in operation as part of the University Politehnica of Bucharest (UPB) campus, which is seen as a single entity in relation with the utility grid having a single point of common coupling (PCC) with the external energy system [73]. The MG operation is divided within 2 buildings: the Electrical Engineering Department Building, MicroDERLab research laboratory (from now on shall be referred to as FEE, i.e., FEE building, FEE side etc.). The work will showcase scenarios of operation for a real test-site having its core infrastructure composed by two microgrids tied together with a DC link, acting as two UniRCon (self-consumption and no power injection into the grid). We shall now call this self-RES consumption community DC link enabled microgrid as **Flexi-MLAB**. A simplified representation is in Figure 4-1. The architecture includes loads with highly variable power profiles (office appliances) available with high time granularity (1s reporting rate), PV panels and a battery energy storage system (BESS) to match, when necessary, the differences between generation and load, while also keeping the voltage level in a narrow (±10%) band.

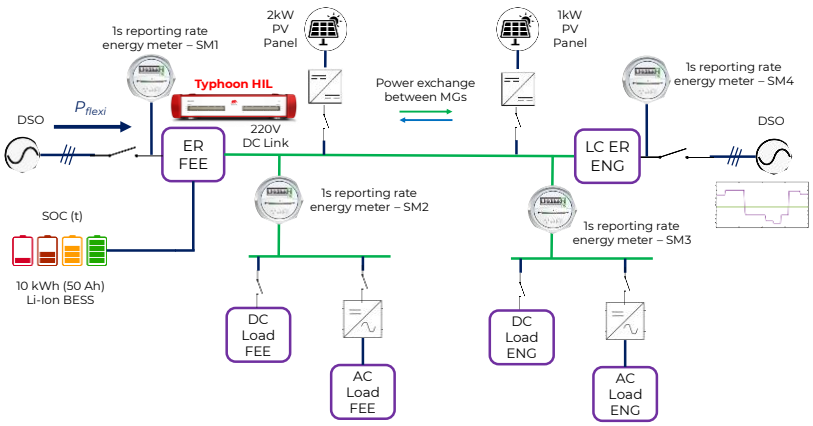

Figure 4-1. Flexi-MLAB simplified grid topology.

4.3 Highly-variable, high-time-granularity load power profiles

To study the behavior and operation of Flexi-MLAB, for the energy consumption side, it has been made use of 1s-reporting rate load profiles derived from high reporting measurements using the so-called Unbundled Smart Meter (USM) concept [107], required for achieving an optimal operation of the proposed emerging system. To be noted that the USM has been based on a DC

energy meter described and used in [3]. The load is composed by specific profiles for office appliances such as personal computers (PCs), TV, refrigerator, air-conditioning and servers. Examples of operation for some of these appliances can be observed in Figure 4-2.

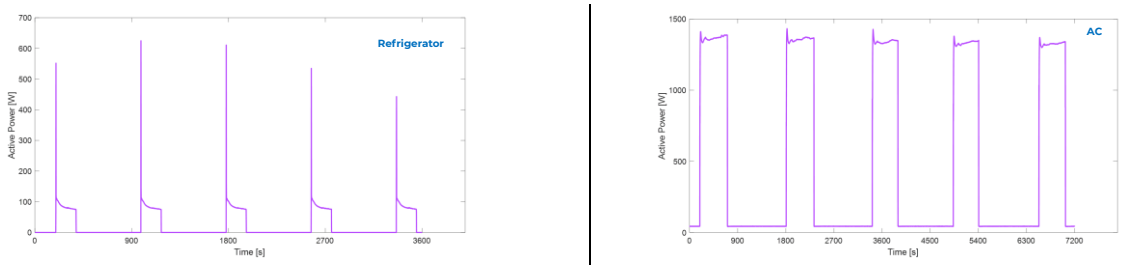

(a) (b)

Figure 4-2. Power profiles for the operation of a (a) refrigerator and (b) air conditioning
Reporting rate 1 frame/second

4.4 Highly variable high-time-granularity PV power generation

Local PV-generation has the power profiles based on daily real data obtained from USM-reported measurements. The profiles were made available with 1s reporting rate and correspond to Flexi-MLAB location in Bucharest.

4.5 Pre-defined power profile with the utility

To achieve a certain degree of operation predictability and flexibility planning, coping with multiple sources of uncertainties at distribution level in the emerging grids, this chapter proposes a solution for pre-defined (pre-agreed) 1h power profiles between the customer and the energy utility. The innovative approach in this regard associated with the paper is the demonstration of possible impact of power contracts based on predefined load profiles and not on rated/approved maximal power. An example of the proposed solution with pre-agreed power profiles aggregated over constant time intervals is given in Figure 4-3.

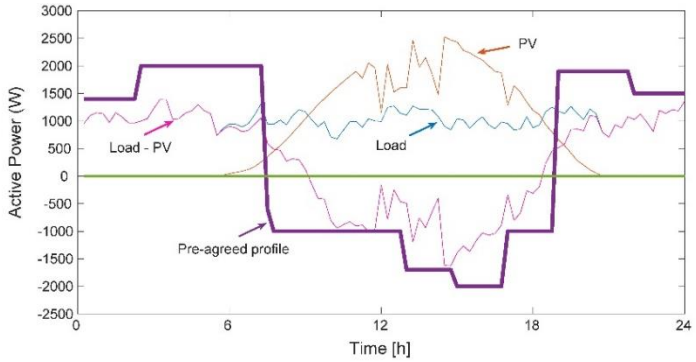

Figure 4-3. Graphical demonstration of the concept for pre-agreed hourly power profiles

4.6 Battery Storage Energy System

As for the Flexi-MLAB to operate in the paradigm of self-consumption (based on the regulatory accepted condition) and to efficiently maximize the PV generation, a battery energy storage system (BESS) is in place and composed of multiple 12V, 3Ah Li-Ion batteries, 10 kWh. The capacity of the battery system has been previously selected based on resilience studies conducted for the FEE building. Formulating regulatory and technical restrictions of operation for Flexi-MLAB in terms of no power injection into the grid, the energy router on FEE side integrating the BESS has to solve

a simple optimization problem to balance loads and PV generation. In this paper the control algorithm relies on controlling solely P_{flexi}. The system does not inject power into the main grid since the total load power is always strictly positive. This power is represented by the difference between generation (PV production and battery, when discharging) and total load (sum of the DC and AC loads on FEE side and ENG side and battery when in charging mode).

4.7 Scenarios for a DC link enabled energy community (with PV)

In our specific case, the scenario used for the prosumer does not take into consideration the power injection into the main network. The operation strategy of the microgrid under analysis in this paper (and described in the next chapter), basically, of consuming the generated PV power by the DC and AC loads. When there is no sufficient irradiance, also power coming from the main grid is required. Given the terms defined in previous sections, the behavior of the microgrid is simulated in the context of the pre-agreed power profiles exchanged with the DSO and operation for two scenarios, normal weekday during summer and normal summer weekend.

4.7.1 The Loads of Flexi-MLAB

4.7.1.1 The AC and DC Loads of Flexi-MLAB – weekend

Total load on FEE side during weekend can be seen in Figure 4-4 over 24h time variation with 1s resolution, real data reported by the energy meter SM2 in Figure 4-1.

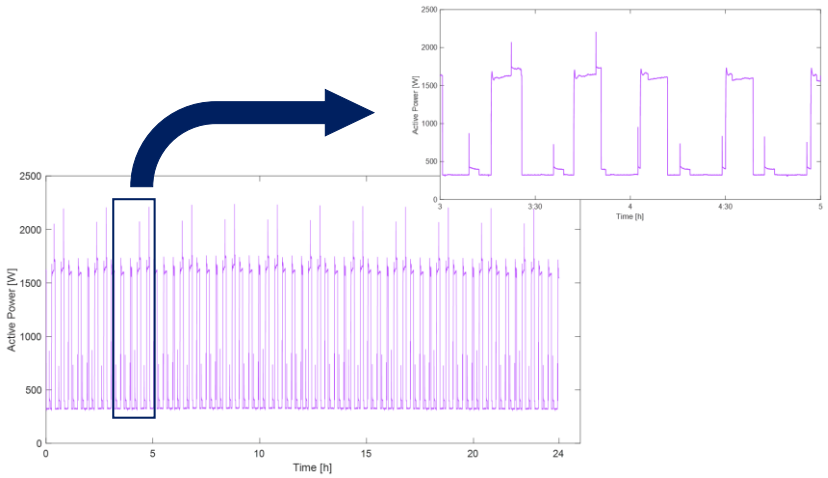

Figure 4-4. Time varying active power over 24h with 1s granularity for the total load on FEE side during weekend.

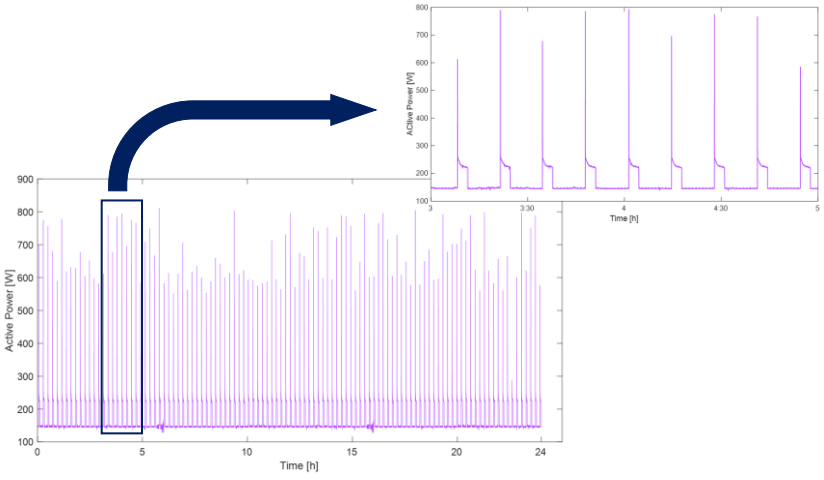

Figure 4-5. Time varying active power over 24h with 1s granularity for the total load on ENG side during the weekend.

Total load on ENG side during the weekend can be seen in Figure 4-5 over 24h time variation, with 1s resolution, real data reported by the energy meter SM3 din Figure 4-1.

4.7.2 PV Generation in Flexi-MLAB

The test system consists of RES-based generation of 2 PV systems, one of 2kW (peak power) on the roof of FEE building and one of 1kW (peak power) on the roof of ENG building (200 m apart). The aggregated power profile over 24h for the PV generation is presented in Figure 4-6.

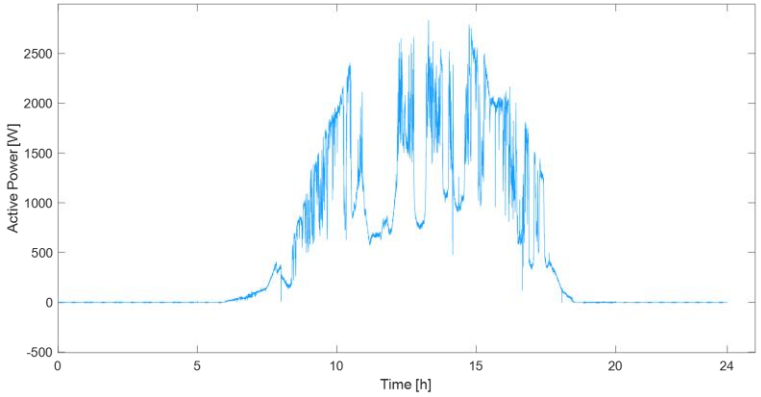

Figure 4-6. Considered PV power profile in summer, 24h, 1s granularity; aggregated for both ENG and FEE installations.

The study was conducted for the worst case scenarios of operation, as defined by keeping $P_{flexi} > 0$, always, which translates to maximal PV generation during minimum loading.

4.7.3 Energy supply

As stated in the previous section, to maximize the effective use of previous knowledge to cope with uncertainty in both generation and loading conditions, contractual pre-agreed power profiles are implemented, with different patterns for weekday and weekend.

4.7.3.1 Predefined contractual power profiles on ENG side – weekend

In Figure 4-7 can be seen the proposed profile during weekend in summer.

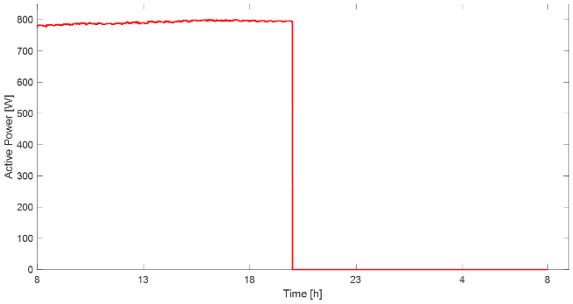

Figure 4-7. Predefined 24h contractual power with the utility grid; weekend in summer

4.8 Typhoon HIL Environment

To study and demonstrate the operation of the proposed test-case SCC, a Typhoon HIL system (HIL402 Series) [159] is used to emulate the parts of the system, including DSO feeder side, distributed generation (solar PV panels), BESS, DC and AC loads, the interconnection DC link and the core of the system, the energy router, as software in the loop (emulating and testing the control algorithms for Flexi-MLAB). The model is built upon real data collection and analytics for high variable power profiles (1s reporting rate), the electrical system being implemented in Typhoon

environment enabling real time data generation and access to data analytics for proper validation using software-in-the-loop experiments.

4.9 Real-Time Simulation and Results

In Typhool HIL 402series, all components and algorithm scripts were integrated and compiled (using schematic editor) and the simulation was carried out in HIL SCADA for a weekday and one weekend day (a total of 48h of simulation) as to capture the real-time operation of Flexi-MLAB. Realtime with software-in-the-loop simulation was carried out to monitor the behaviour of the MG in the cases described above.

4.9.1 Case 1. Weekend scenario

For the weekend, when loading conditions are lower, it can be seen the better use of battery capacity (Figure 4-8) under the same smoothing characteristics (P_{flexi} in Figure 4-9) following the energy exchange on DC-link (Figure 4-10).

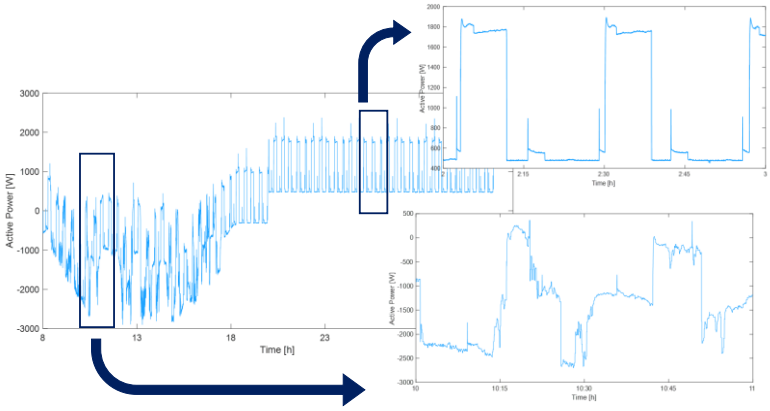

Figure 4-8. Time varying active power over 24h with 1s granularity for the BESS system during a normal weekend day

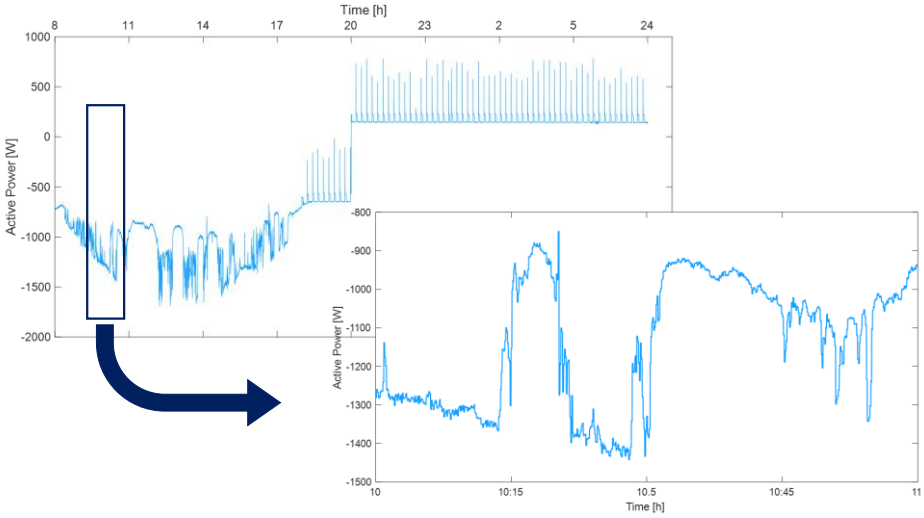

Figure 4-9. Time varying active power over 24h with 1s granularity exchanged on the internal DC link during a normal weekend day.

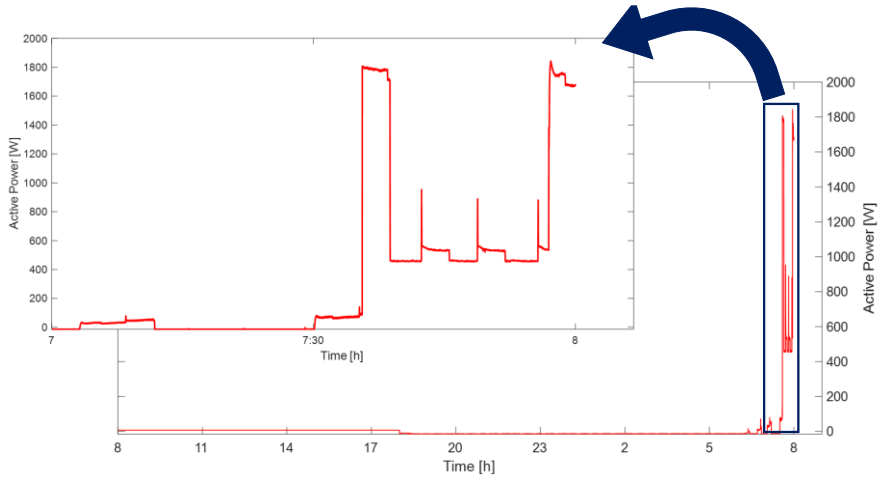

Figure 4-10. Time varying active power over 24h with 1s granularity supplied on FEE grid side during a normal weekend day.

4.10 Introduction for real-time digital simulations and Typhoon HIL technology

Typhoon HIL is a real-time digital simulator (allowing *hardware-in-the-loop* si *software in the loop* experiments), for advanced testing and development tools for a wide range of applications. These simulators are specifically designed to provide users with a high-fidelity, real-time platform for developing and testing complex systems, including power electronics, microgrids, and renewable energy systems. The Typhoon HIL real-time simulator also includes a powerful simulation software package, which provides a wide range of tools for designing, testing, and analyzing complex systems. The software includes a user-friendly graphical interface, which makes it easy to set up simulations and analyze results. Typhoon HIL that is based on a real-time circuit simulation algorithm and a high-throughout, low-latency processor architecture implemented in a field programmable gate array (FPGA). The FPGA architecture is scalable and could function in multiple configurations that interconnect Standard Processing Cores (SPCs), machine solver, look-up-tables, PWM modulator etc. The configuration and characteristics used are for a HIL402. The figure below showcases Typhoon HIL Control Center with its main software components.

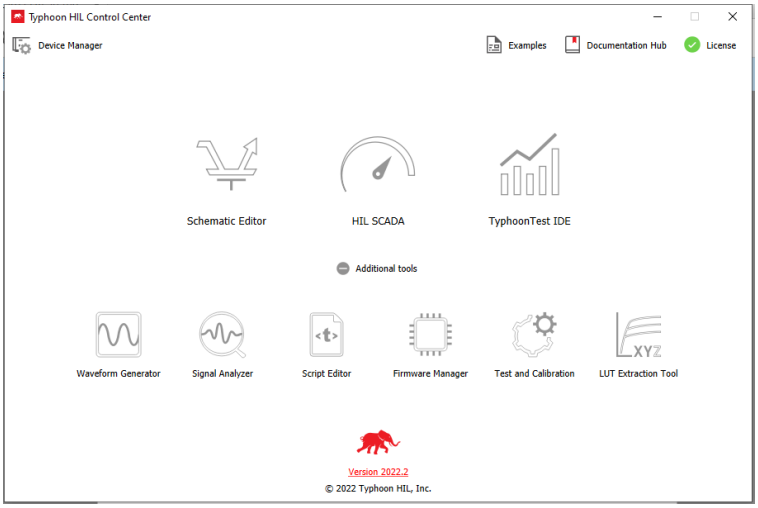

Figure 4-11. Typhoon HIL Control Center

5 Conclusions and personal contributions

5.1 Conclusions

The assessment of emerging low-inertia power systems is a critical task for ensuring the stability and reliability of the power grid in the face of increasing renewable energy penetration. As more variable renewable energy sources, such as wind and solar, are added to the grid, the system inertia is decreasing, and new challenges are emerging. To address these challenges, new approaches are needed for modeling, simulation, and control of low-inertia power systems. Advanced tools, such as real-time simulators, can be used to test and evaluate the performance of these systems under different operating conditions and disturbances.

It is important to develop new methods for control strategies that can effectively manage the variability and uncertainty of renewable energy sources and maintain system stability. These strategies may include the use of energy storage systems, flexible power electronics, and advanced control algorithms.

The method proposed in this paper is based on two different methods that were adapted and improved: The enhanced Hilbert–Huang method based on masking signals for identification of oscillation modes existing in distorted time-varying waveform and the synthesis of a steady-state signal as presented in the QSSI algorithm. The abilities of the original HH and of the improved versions were demonstrated for time-frequency and time-amplitude localization and the importance of masking signals to enhance EMD for power quality applications. The proposed hybrid HH showed efficiency in separation of modes of oscillation that only evolve on certain time intervals inside the investigation window. The advantages of the method were under-lined and explained above, but the optimal illustration was made using signals for which the identification of change of steady state is hard to achieve. For those type of signals, unusual components (such as 430 Hz and 494 Hz) with time-varying amplitudes were added, and the method successfully identified them. The goal of dividing the original signal into quasi-steady-state time intervals was successfully achieved as the last step of the hybrid method, giving the opportunity of achieving a detailed time–frequency description of the signal and, as such, of identifying the underlining phenomena to be further addressed by appropriate design and control schemes. Moreover, the results of QSSI can be helpful in many applications where steady-state assumption is crucial (e.g., state estimation). Another important direction for QSSI is for load and generation signature profiling by studying the distorted time-varying power waveforms at the Point of Common Coupling for low-voltage prosumers distribution grids. The method was tested on two case studies, one with a synthetic digitized waveform and the other with actual current waveform measure-ments specific for a microwave oven operation.

Knowledge extraction and information loss, in case of daily load power profiles of UPB student campus buildings can be achieved by high reporting rate measurements and accurate models of the energy transfer. In this paper we use averaged power profiles instead of those obtained from smart meters with 0.5 frames/s time reporting rate derived from extensive local measurements using Unbundled Smart Meters (USM), set on 1s reporting rates. the information loss variation for all the cases studied and described in this paper. The use-cases studied for winter and summer, weekday, and weekend day for temporal and spatial aggregation 30 rooms and 1500 students and 150 rooms and 300 students for summer and winter, for weekdays and weekends and aggregation over 1-min, 15-min and 1-h, single-phase and three-phase. The thesis shows the benefits of extracting relevant technological information from high-reporting rate smart meters using simple to calculate statistical metrics able to preserve user privacy, while observing, offline, the system behavior within the same reporting rates as per current industry standards. This work proposed a general

knowledge extraction framework, with a focus on a statistical based methodology which aims to mitigate dual constraints coming from smart meter data owners (privacy and cyber security concerns) and from the needs of the DSO to enhance the network situational awareness down to the most remote parts of its LV network in order to ensure reliability and high quality of service. The proposed statistical metrics to satisfy these constraints are the percentiles (e.g., p95 and p99) and the cumulative probability function (cdf). They are simple enough to be processed and encrypted at SM level using the same processing unit, while capturing relevant system dynamics within the time window between two consecutive reporting moments as per the current industry standard (usually 15- or 60-min aggregation).

Two laboratories with prosumer behavior in the UPB campus have been interconnected via a 220V DC link to ensure optimal operation of the resulting microgrid, ensuring a load-only power profile. Numerical simulations have been done in a Typhoon HIL real-time environment where the grid information and control signals are available using 1s time-resolution data. Power profiles for load and PV generation during weekday and weekend have been derived from historical real time measurements using unbundled smart meter with 1s time granularity. The flexibility for the entire microgrid was provided by the shared storage unit and the power exchanged between the prosumers via DC link. Real time numerical simulations have been conducted for 24h continuous operation in each of the two worse-case scenarios (weekday/weekend). Regulatory constraints have been modeled by compulsory no-infeed operation and preset load profiles in PCC, with step-wise hourly resolution. The control algorithm shows the feasibility of such arrangement and the advantage of cancelling the power variability (negative impact for the utility) by exploiting the flexibility brought by DC link in the proposed set-up. Results have been obtained using the Typhoon Real-time simulation environment.

5.2 Personal contributions

- **Low-inertia emerging power systems.** By studying the bibliography and specialized literature and by analyzing the different classification systems and definitions proposed by other researchers, in this thesis the challenges that must be addressed for a complete understanding of the operation and functioning of microgrids were identified and evaluated, especially from the perspective of the associated regulations and standards. Several research directions have been identified and studied that can contribute to the development of the context and exploitation of microgrids, such as the development of new methods of power transfer analysis and new variables for evaluating the visibility and development of microgrids, exploring the potential of new technologies and evaluating the impact microgrids on the public distribution network but also on society. Another important aspect discussed is related to the need for measurements with a high reporting rate in the assessment and monitoring of energy transfer in microgrids, where locally distributed generation has a high degree of unpredictability, energy use has a highly variable character and the control of the operation of microgrids requires implementation and coordination of flexibility strategies.
- **Time-frequency analysis for voltage and current waveforms.** The method proposed in this paper is based on two different methods that were adapted and improved: The enhanced Hilbert–Huang method based on masking signals for identification of oscillation modes existing in distorted time-varying waveform and the synthesis of a steady-state signal as presented in the QSSI algorithm. The abilities of the original HH and of the improved versions were demonstrated for time-frequency and time-amplitude localization and the importance of masking signals to enhance EMD for power quality applications. The proposed hybrid HH showed efficiency in separation of modes of oscillation that only

evolve on certain time intervals inside the investigation window. The advantages of the method were under-lined and explained above, but the optimal illustration was made using signals for which the identification of change of steady state is hard to achieve. For those type of signals, unusual components (such as 430 Hz and 494 Hz) with time-varying amplitudes were added, and the method successfully identified them. The goal of dividing the original signal into quasi-steady-state time intervals was successfully achieved as the last step of the hybrid method, giving the opportunity of achieving a detailed time–frequency description of the signal and, as such, of identifying the underlining phenomena to be further addressed by appropriate design and control schemes. Moreover, the results of QSSI can be helpful in many applications where steady-state assumption is crucial (e.g., state estimation). Another important direction for QSSI is for load and generation signature profiling by studying the distorted time-varying power waveforms at the Point of Common Coupling for low-voltage prosumers distribution grids. The method was tested on two case studies, one with a synthetic digitized waveform and the other with actual current waveform measurements specific for a microwave oven operation and the results were compared with the results from a power quality analyzer ELSPEC G4430.

- **Information loss associated with low reporting rates for measurement data.** Knowledge extraction and information loss, in case of daily load power profiles of UPB student campus buildings can be achieved by high reporting rate measurements and accurate models of the energy transfer. In this paper we use averaged power profiles instead of those obtained from smart meters with 0.5 or 1 frames/second time reporting rate derived from extensive local measurements using Unbundled Smart Meters (USM).
- **High reporting rate smart metering data infrastructure for low-inertia power systems.** The thesis shows the benefits of extracting relevant technological information from high-reporting rate smart meters using simple to calculate statistical metrics able to preserve user privacy, while observing, offline, the system behavior within the same reporting rates as per current industry standards. This work proposed a general knowledge extraction framework, with a focus on a statistical based methodology which aims to mitigate dual constraints coming from smart meter data owners (privacy and cyber security concerns) and from the needs of the DSO to enhance the network situational awareness to ensure reliability and high quality of service.
- **Real-time digital simulations using Typhoon HIL technology.** To study and demonstrate the operation of the proposed test-case of a microgrid, reducing the costs of both users and utility by eliminating bi-directional power flow and increase the generation from renewable energy sources, ensuring energy balance, reliability and awareness over the power profiles, system software and hardware elements that provides access to real-time data and microgrid decision making are required. A Typhoon HIL system (HIL402 Series) is used to emulate the parts of the system, including DSO feeder side, distributed generation (solar PV panels), BESS, DC and AC loads, the interconnection DC link and the core of the system, the energy router, as software in the loop (emulating and testing the control algorithms for Flexi-MLAB). The model is built upon real data collection and analytics for high variable power profiles (1s reporting rate), the electrical system being implemented in Typhoon environment enabling real time data generation and access to data analytics for proper validation. The files, as collected on site, containing 1s resolution power profiles (load and generation) were imported in Typhoon HIL and served as inputs (using read from file feature) for the blocks used in the schematic editor. Dedicated widgets for data acquisition

were deployed in the HIL SCADA (Typhoon HIL special environment for running the simulation) for making use of 1s resolution results.

- **Predefined contractual power profiles.** To achieve a certain degree of operation predictability and flexibility planning, coping with multiple sources of uncertainties at distribution level in the emerging grids, this paper proposes a solution for pre-defined (pre-agreed) 1h power profiles between the customer and the energy utility. One of the objectives of the work reported in this paper is to validate solutions tailored for the energy transfer variability for both demand and prosumers RES-based generation, thus solving the issues derived from planning and operation uncertainty. In the thesis the use was for load and generation models derived from extensive local measurements using Unbundled Smart Meters (USM), set on 1s reporting rates. Focus has been on the flexibility provided by the interplay of the active elements in the DC-link enabled microgrid.

Bibliography

[1]. A. Correa-Florez, A. Michiorri and G. Kariniotakis, "Optimal Participation of Residential Aggregators in Energy and Local Flexibility Markets," in IEEE Transactions on Smart Grid, vol. 11, no. 2, pp. 1644-1656, March 2020.

[2]. A.N. Zomers, "The Electrification Challenge", Cape Town CIGRE/IEC Symposium, October 2015.

[3]. Albu, E. Kyriakides, G. Chicco, M. Popa and A. Nechifor, "Online Monitoring of the Power Transfer in a DC Test Grid," in IEEE Transactions on Instrumentation and Measurement, vol. 59, no. 5, pp. 1104-1118, May 2010.

[4]. Amoud, H.; Snoussi, H.; Hewson, D.J.; Duchene, J. Hilbert-Huang Transformation: Application to Postural Stability Analy-sis. In Proceedings of the 2007 29th Annual International Conference of the IEEE Engineering in Medicine and Biology So-ciety, Lyon, France, 22–26 August 2007, pp. 1562–1565.

[5]. An ICT platform for Sustainable Energy Ecosystem in Smart Cities, ERANET-LAC-ITCITY, NR. 23/2017, http://itcity.microderlab.pub.ro/

[6]. Andres Felipe Martinez Palomino – Study of Acceptability Curve of in use appliances directly supplied by DC Microgrid, Master Thesis - Politecnico din Torino, 2016.

[7]. Anxu, "On quantitative identification of explosion earthquake based on cepstrum computation of HHT and statistical simulation of sub-cluster," in Chinese Control Conference, Hefei, 2012.

[8]. Assessment of standard voltages and power quality requirements, en

[9]. Ayon, J.K. Gruber, B.P. Hayes, J. Usaola, M. Prodanovic, "An optimal day-ahead load scheduling approach based on the flexibility of aggregate demands", Appl. Energy. 198 (2017) pp.1-11.

[10]. Baayeh, A.G.; Bayati, N. Adaptive Overhead Transmission Lines Auto-Reclosing Based on Hilbert–Huang Transform. En-ergies 2020, 13, 5416.

[11]. Backhaus, G. W. Swift, S. Chatzivasileiadis, W. Tschudi, S. Glover, M. Starke et al., DC Microgrids Scoping Study—Estimate of Technical and Economic Benefits, Los Alamos National Laboratory, March 2015.

[12]. Baringo, R. Sanchez-Amaro, "A stochastic robust optimization approach for the bidding strategy of an electric vehicle aggregator", Electr. Power Syst. Res. 146 (2017) 362–370.

[13]. Bayer, P. Matschoss, et al., 'The German experience with integrating photovoltaic systems into the low-voltage grids', Renewable Energy, vol. 119, pp. 129–141, Apr. 2018.

[14]. BeagleBone Black low-cost, community-supported development platform for developers and hobbyists. [Online] disponibil: https://beagleboard.org/black

[15]. Belanger, P. Venne, J.-N. Paquin, "The What, Where and Why of Real-Time Simulation, IEEE 2003.

[16]. C. Sharpley and V. Vatchev, "Analysis of intrinsic mode functions," Industrial Mathematics Institute Research Report 2004, Dept. Math., Univ. South Carolina, 2004.

[17]. Chicco, P. Mancarella, Distributed multi-generation: a comprehensive view, Renewable and Sustainable Energy Reviews, 13 (3) (2009), pp. 535-551

[18]. Chilukuri, M.V.; Dash, P.K. Multiresolution S-Transform-Based Fuzzy Recognition System for Power Quality Events. IEEE Trans. Power Deliv. 2004, 19, 323–330.

[19]. Christoforidis, Georgios C. and Panapakidis, Ioannis P. and Papadopoulos, Theofilos A. and Papagiannis, Grigoris K. and Koumparou, Ioannis and Hadjipanayi, Maria and Georghiou, George E. – A Model for the Assessment of Different Net-Metering Policies, Energies, 2016, https://www.mdpi.com/1996-1073/9/4/262

[20]. CIGRE Technical Brochure 635 (2015) Microgrids 1: Engineering, Economics & Experiences, WG C6.22, www.e-cigre.org; ISBN 978-2-85873-338-5

[21]. CIGRE Working Group C.22). Microgrids 1, Engineering, Economics, & Experience. Paris, France. Ref. 635, October; 2015 http://www.e-cigre.org/publication/635-microgrids-1-engineering–economics–experience.

[22]. Çimen, Halil, Çetinkaya, Nurettin and Vasquez, Juan C. and Guerrero, Josep M. – A Microgrid Energy Management System Based on Non-Intrusive Load Monitoring via Multitask Learning, IEEE Transactions on Smart Grid, 2021.

[23]. Ciornei, Irina and Albu, Mihaela and Sanduleac, Mihai and Rodriguez-Diaz, Enrique and Guerrero, Josep and Vásquez, Juan C. – {Real-time optimal scheduling for prosumers resilient to regulatory changes, 2018 IEEE International Energy Conference (ENERGYCON).

[24]. Ciornei, Irina and Albu, Mihaela and Sănduleac, Mihai and Rodriguez-Diaz, Enrique and Teodorescu, Remus and Guerrero, Josep – Adaptive Distributed EMS for Small Clusters of Resilient LVDC Microgrids, 2018 IEEE International Conference on Environment and Electrical Engineering and 2018 IEEE Industrial and Commercial Power Systems Europe (EEEIC / I CPS Europe).

[25]. Ciornei, L. Hadjidemetriou, M. Albu, M. Sanduleac, E.Kyriakides, "Analytical derivation of PQ indicators compatible with control strategies for DC microgrids," IEEE PowerTech, Manchester, UK, 18-22 June 2017.

[26]. Cohen, L. Time frequency distributions—A review. Proc. IEEE 1989, 77, 941–981.

[27]. Cui, Zhicheng, Wenlin Chen, and Yixin Chen. "Multi-scale convolutional neural networks for time series classification." arXiv preprint arXiv:1603.06995 (2016).

[28]. Dash, P.K.; Panigrahi, B.K.; Panda, G. Power quality analysis using s-transform. IEEE Trans. Power Deliv. 2003, 18, 406–411.

[29]. Deering and J. F. Kaiser, "The use of masking signal to improve empirical mode decomposition," in Proc. IEEE Int. Conf. Acoustics, Speech Signal Processing (ICASSP'05), 2005, vol. 4, pp. 485–488.

[30]. Deering, R.; Kaiser, J.F. The use of masking signal to improve empirical mode decomposition. In Proceedings of the IEEE International Conference Acoustics, Speech Signal Processing (ICASSP'05), Philadelphia, PL, USA, 22–23 Mach 2005, vol. 4, pp. 485–488.

[31]. Denholm, M. O'Connell, et al. – Overgeneration from Solar Energy in California. A Field Guide to the Duck Chart, NREL, Denver USA, Technical Report NREL/TP-6A20-65023, Nov. 2015.

[32]. Dowling, Alexander W., Ranjeet Kumar, and Victor M. Zavala. "A multi-scale optimization framework for electricity market participation." Applied Energy 190 (2017): 147-164.

[33]. Dreidy M, Mokhlis H, Mekhilef S. Inertia response and frequency control techniques for renewable energy sources: a review. Renew Sustain Energy Rev 2017;69:144–55.

[34]. Driesen, J., Craenenbroeck, T.V., Reekmans, R., Dommelen, D.V. Analysing time-varying power system harmonics using wavelet transform. In Proceedings of the IEEE Instrumentation and Measurement Technology Conference, Brussels, Bel-gium, 4–6 June 1996.

[35]. E Huang, N.; Shen, S.S.P. Hilbert-Huang Transform and Its Applications; World Scientific: Singapore, 2005.

[36]. E. Huang and S. S. P. Shen, Eds., Hilbert-Huang Transform and Its Applications. Singapore: World Scientific, 2005.

[37]. ELSPEC—Where Power meets Quality. Available online: https://www.elspec-ltd.com/metering-protection/power-quality-analyzers/g4400-power-quality-analyzer/ (accessed on 17 March 2021).

[38]. EPRI (Electric Power Research Institute). 2019. Meeting the Challenges of Declining System Inertia, 3002015131 April 2019

[39]. Eremia, M., & Shahidehpour, M. (Eds.). (2013). Handbook of electrical power system dynamics: modeling, stability, and control. John Wiley & Sons.

[40]. Eto, Joseph H., John Undrill, Ciaran Roberts, Peter Mackin, and Jeffrey Ellis. 2018. Control Requirements for Reliable Interconnection Frequency Response. Lawrence Berkeley National Laboratory. LBNL-2001103. Disponibil online: https://eta-publications.lbl.gov/sites/default/files/frequency_control_requirements_lbnl-2001103.pdf

[41]. F. Locment and M. Sechilariu, "Modeling and Simulation of DC Microgrids for Electric Vehicle Charging Stations," Energies, vol. 8, no. 5, pp. 4335, May 2015.

[42]. Faraji, Jamal and Ketabi, Abbas and Hashemi-Dezaki, Hamed – Optimization of the scheduling and operation of prosumers considering the loss of life costs of battery storage systems, The Journal of Energy Storage.

[43]. Fawaz, Hassan Ismail, et al. "InceptionTime: Finding AlexNet for Time Series Classification." arXiv preprint arXiv:1909.04939 (2019).

[44]. Frieden, Dorian and Tuerk, Andreas and Neumann, Camilla and d'Herbemont, Stanislas and Roberts, Joshua, Collective self-consumption and energy communities: Trends and challenges in the transposition of the EU framework, December 2022.

[45]. G. Phadke, "Synchronized phasor measurements in power systems," IEEE Computer Applications in Power, pp. 10-15, Apr. 1993.

[46]. G. Phadke, J. S. Thorp and M. G. Adamiak, "A new measurement technique for tracking voltage phasors, local system frequency, and rate of change of frequency," IEEE Trans. Power Apparatus and Systems, vol. PAS-102, No. 5, pp. 1025 - 1038, 1983.

[47]. G. Rilling, P. Flandrin and P. Goncalves, "On empirical decomposition and its algorithms," in IEEE-EURASIP Workshop on Nonlinear Signal Image Process, Grado, Italy, 2003.

[48]. G. Stamatescu, R. Entezari, K. Römer and O. Saukh, "Deep and Efficient Impact Models for Edge Characterization and Control of Energy Events," 2019 IEEE 25th International Conference on Parallel and Distributed Systems (ICPADS), Tianjin, China, 2019, pp. 639-646.

[49]. G. Stamatescu, **R. Plamanescu**, I. Ciornei and M. Albu, "Detection of Anomalies in Power Profiles using Data Analytics," 2022 IEEE 12th International Workshop on Applied Measurements for Power Systems (AMPS), Cagliari, Italy, 2022, pp. 1-6.

[50]. G. T. Heydt, P. S. Field, C. C. Liu, D. Pierce, L. Tu, and G. Hensley, "Applications of the windowed FFT to electric power quality assessment," IEEE Trans. Power Del., vol. 14, no. 4, pp. 1411–1416, Oct.1999.

[51]. G. Van den Broeck, T. D. Mai, and J. Driesen, "MatLVDC: A New Open Source Matlab Toolbox to Simulate DC Networks including Power Electronic Converters and Distributed Energy Resources," IEEE Power and Energy Society General Meeting, Denver, USA, pp. 1-4, 26-31 July 2015.

[52]. Galli, A.; Heydt, G.; Ribeiro, P. Exploring the power of wavelet analysis. IEEE Comput. Appl. Power 1996, 9, 37–41.

[53]. Ghosal et al., "Key management systems for smart grid advanced metering infrastructure: A Survey," in IEEE Communications Surveys & Tutorials, vol. 21, no. 3, pp. 2831-2848, 2019.

[54]. Green, M. Prodanovic Control of inverter-based micro-grids Electric Power Systems Research, 77 (9) (2007), pp. 1204-1213

[55]. Griffel, B.; Calvano, S.E.; Coyle, S.M.; Macor, M.A.; Jan, B.U.; Reddell, M.; Semmlow, J.L.; Corbett, S.; Lowry, S.F. Instan-taneous frequency analysis shows greater sensitivity to parasympathetic components of heart rate than spectral analysis. In Proceedings of the 2013 IEEE Signal Processing in Medicine and Biology Symposium (SPMB), Brooklyn, NY, USA, 7 December 2013, pp. 1–5.

[56]. H. Kirkham and M. Albu, "Measurement, Nyquist and Shannon: A view of PMU metrology," 2017 10th International Symposium on Advanced Topics in Electrical Engineering (ATEE), Bucharest, 2017, pp. 23-27.

[57]. H. Kirkham and R. White, "The Modern Measurement Challenge," 2019 IEEE International Instrumentation and Measurement Technology Conference (I2MTC), Auckland, New Zealand, 2019, pp. 1-6.

[58]. H. Liang, Q. H. Lin and J. D. Z. Chen, "Application of the empirical mode decomposition to the analysis of esophageal manometric data in gastro-esophageal reflux disease," IEEE Trans. Biomed. Eng, vol. 52, no. 10, p. 1692–1701, 2005.

[59]. Hatziargyriou, Nikos, Microgrids: architectures and control, ed. John Wiley & Sons, 2014.

[60]. https://www.typhoon-hil.com/

[61]. Huang, B. Kasztenny, V. Madani, K. Martin, S. Meliopoulos, D. Novosel and J. Stenbakken, "Performance evaluation of phasor measurement systems," in Proc. IEEE Power Engineering Society General Meeting, Pittsburgh, PA, pp. 1-7, July 2008.

[62]. Huang, N.E. The empirical mode decomposition and the Hilbert spectrum for nonlinear and non-stationary time series analysis. In Proceedings of the Royal Society of London, Royal Society, London, UK. ; volume 454, no. 1971, pp. 903—995, March 1998.

[63]. IEC 61000-4-30 Electromagnetic compatibility (EMC) Part 4-30: Testing and measurement techniques - Power quality measurement methods

[64]. IEC 62056-1-0:2014, "Electricity metering data exchange – the dlms/cosem suite - part 1-0: Smart metering standardisation framework,"2014

[65]. IEC International Electrotechnical Commission. IEC 61000-4-30 (edition 3.0: 2015, COR1:2016). In Electromagnetic compatibility (EMC)—Part 4–30: Testing and Measurement Techniques—Power Quality Measurement Methods; IEC International Electrotechnical Commission: Geneva, Switzerland, 2016.

[66]. IEC TR 63282:2020 – Technical Report – LVDC systems - Assessment of standard voltages and power quality requirements, TC8 – 2020.

[67]. IEEE Guide for Phasor Data Concentrator Requirements for Power System Protection, Control, and Monitoring, IEEE Standard C37.244-2013

[68]. IEEE Guide for Synchronization, Calibration, Testing, and Installation of Phasor Measurement Units (PMUs) for Power System Protection and Control, IEEE Standard C37.242-2013

[69]. IEEE Guide for the Interpretation of Gases Generated in Mineral Oil-Immersed Transformers', IEEE Std C57.104-2019, Piscataway, NJ, USA, 2019, pp. 1–98.

[70]. IEEE Standard for Synchrophasor Measurements for Power Systems -- Amendment 1: Modification of Selected Performance Requirements," in IEEE Std C37.118.1a-2014 (Amendment to IEEE Std C37.118.1-2011) , vol., no., pp.1-25, 30 April 2014.

[71]. IEEE standard for synchrophasors for power systems, IEEE Standard 1344-1995.

[72]. IEEE standard for synchrophasors for power systems, IEEE Standard C37.118-2005.

[73]. IEEE Standard for the Specification of Microgrid Controllers 2018, IEEE Std 2030.7-2017.

[74]. IEEE/IEC International Standard - Measuring relays and protection equipment - Part 118-1: Synchrophasor for power systems - Measurements," in IEC/IEEE 60255-118-1:2018, vol., no., pp.1-78, 19 Dec. 2018.

[75]. Intelligent FIWARE-based Generic Energy Storage Services for Environmentally Responsible Communities and Cities, joint programming initiative MiCall19, project number 176 - ERANET-REGSYS-I-GRETA, http://i-greta.microderlab.upb.ro/

[76]. International Electrotechnical Commission, "CISPR 16/TR 16-3: Specification for radio disturbance and immunity measuring apparatus and methods - Part 3: CISPR technical reports,"

[77]. International Electrotechnical Commission, "CISPR 16-1-1: Specification for radio disturbance and immunity measuring apparatus and methods - Part 1-1: Radio disturbance and immunity measuring apparatus - Antennas and test sites for radiated disturbance measurements,"

[78]. International Electrotechnical Commission, "IEC 61000-4-7: Electromagnetic Compatibility (EMC) – Part 4-7: Testing and measurement techniques – General guide on harmonics and interharmonics measurements and instrumentation, for power supply systems and equipment connected thereto," 2021.

[79]. Irina Ciornei, Mihaela Albu, Mihai Sanduleac, Enrique Rodriguez-Diaz, Josep M. Guerrero, Juan C. Vasquez, 2018, Real-time optimal scheduling for prosumers resilient to regulatory changes, Proc. of the 2018 IEEE International Energy Conference (ENERGYCON), Limassol, CYPRUS, Jun 03-07, 2018.

[80]. J. C. Nunes, Y. Bouaoune, E. Delechelle, N. Oumar and P. Bunel, "Image analysis by bidimensional empirical mode decomposition," Image Vis. Comput., vol. 21, p. 1019–1026, 2003.

[81]. J. Driesen, T. V. Craenenbroeck, R. Reekmans, and D. V. Dommelen, "Analysing time-varying power system harmonics using wavelet transform," in Proc. IEEE Instrumentation and Measurement Technology Conf., 1996.

[82]. J. Guerrero, J. Vasquez, R. Teodorescu Hierarchical control of droop-controlled dc and ac microgrids: a general approach towards standardization IEEE Industrial Electronics (IECON) (2009), pp. 4305-4310

[83]. J. Jimeno, J. Anduaga, J. Oyarzabal, A. de Muro Architecture of a microgrid energy management system European Transactions on Electrical Power, 21 (2) (2011), pp. 1142-1158

[84]. J. Li, C. Zhao and H. Su, "A mode mixing elimination method of HHT in fault detection," in 2016 2nd International Conference on Cloud Computing and Internet of Things (CCIOT), Dalian, 2016.

[85]. J. von Appen, T. Stetz, M. Braun and A. Schmiegel, "Local Voltage Control Strategies for PV Storage Systems in Distribution Grids," in IEEE Transactions on Smart Grid, vol. 5, no. 2, pp. 1002-1009, March 2014.

[86]. Jiao, S. Yang, Y. Chang, G. Yan and J. Hu, "Detecting a cracked rotor with HHT-based time-frequency representation," in 2008 IEEE International Conference on Automation and Logistics, Qingdao, 2008.

[87]. Joint Committee for Guides in Metrology, WG 1, "GUM: Guide to the expression of uncertainty in measurement," 2008.

[88]. K. Dash, B. K. Panigrahi, and G. Panda, "Power quality analysis using S-transform," IEEE Trans. Power Del., vol. 18, no. 2, pp. 406–411, Apr. 2003.

[89]. Kamala Sarojini Ratnam, K. Palanisamy, Guangya Yang, Future low-inertia power systems: Requirements, issues, and solutions - A review, Renewable and Sustainable Energy Reviews, Volume 124, 2020, 109773.

[90]. Katiraei, R. Iravani, N. Hatziargyriou, A. Dimeas Microgrids management IEEE Power and Energy Magazine, 9 (5) (2011), pp. 54-65

[91]. Kirkham and A. Riepnieks, "Dealing with non-stationary signals: Definitions, considerations and practical implications," 2016 IEEE Power and Energy Society General Meeting (PESGM), Boston, MA, 2016, pp. 1-5.

[92]. Kotsonias, M. Asprou, et. al., 'State Estimation for Distribution Grids With a Single-Point Grounded Neutral Conductor', IEEE Transactions on Instrumentation and Measurement, vol. 69, no. 10, pp. 8167–8177, Oct. 2020.

[93]. L. Cohen, "Time frequency distributions—A review," Proc. IEEE, vol. 77, no. 7, pp. 941–981, Jul. 1989.

[94]. L. Lijun, S. Yi and W. Yan, "Radar signal filter design base on HHT method," in 31st Chinese Control Conference, Hefei, 2012.

[95]. L. Shengqing, Z. Huanyue, X. Wenxiang and L. Weizhou, "A Harmonic Current Forecasting Method for Microgrid HAPF Based on the EMD-SVR Theory," in 2013 Third International Conference on Intelligent System Design and Engineering Applications, Hong Kong, 2013.

[96]. L. Zhang, J. Zhang, and Y. H. Hu, 'A Privacy-Preserving Distributed Smart Metering Temporal and Spatial Aggregation Scheme', IEEE Access, vol. 7, pp. 28372–28382, 2019.

[97]. Landis+Gyr E550, "Transformer connected commercial electricity meter suitable for low and medium voltage applications," 2022. [Online] Disponibil: https://www.landisgyr.eu/product/landisgyr-e550/

[98]. Li, D.; Ukil, A.; Satpathi, K.; Yeap, Y.M. Hilbert-Huang Transform Based Transient Analysis in VSC Interfaced DC System. IEEE Trans. Ind. Electron. 2020.

[99]. Li, P.; Fei, L.; Qian, J.; Chen, J.; Li, X. Based on the improved HHT and its application in the power quality detection of microgrid. In Proceedings of the 2011 International Conference on Electrical Machines and Systems, Beijing, China, 20–23 August 2011.

[100]. Li, P.; Fei, L.; Xi, P.; Jie, J.; Zhang, J. HHT based on the LS-SVM and its application in the voltage flicker and harmonic detection of microgrid. In Proceedings of the 2011 4th International Conference on Electric Utility Deregulation and Re-structuring and Power Technologies (DRPT), Weihai, Shandong, 6 July 2011.

[101]. M. Albu, M. Sănduleac, and C. Stănescu, 'Syncretic Use of Smart Meters for Power Quality Monitoring in Emerging Networks', IEEE Transactions on Smart Grid, vol. 8, no. 1, pp. 485–492, Jan. 2017.

[102]. M. Asprou, E. Kyriakides, Mihaela Albu, 2012, The Effect of Parameter and Measurement Uncertainties on Hybrid State Estimation, Proc. of the IEEE Power Engineering Society General Meeting, San Diego, CA, U.S.A., 22-26 July 2012, pp. 1-8.

[103]. M. Di Somma, G. Graditi and P. Siano, "Optimal Bidding Strategy for a DER Aggregator in the Day-Ahead Market in the Presence of Demand Flexibility," in IEEE Transactions on Industrial Electronics, vol. 66, no. 2, pp. 1509-1519, Feb. 2019.

[104]. M. Dong; P. C. M. Meira, et. al.,"Non-Intrusive Signature Extraction for Major Residential Loads," IEEE Trans. on Smart Grid, vol. 4, no. 3, pp. 1421 - 1430, Sept. 2013.

[105]. M. H. J. Bollen and I. Y. H. Guo, Signal Processing of Power Quality Disturbances. New York: Wiley, 2006, p. 314.

[106]. M. Pau et al., 'Design and Accuracy Analysis of Multilevel State Estimation Based on Smart Metering Infrastructure', IEEE Transactions on Instrumentation and Measurement, vol. 68, no. 11, pp. 4300–4312, Nov. 2019.

[107]. M. Sanduleac, L. Pons, G. Fiorentino, R. Pop and M. Albu, "The unbundled smart meter concept in a synchro-SCADA framework," 2016 IEEE International Instrumentation and Measurement Technology Conference Proceedings, Taipei, Taiwan, 2016, pp. 1-5.

[108]. M. Sănduleac, I. Ciornei, L. Toma, **R. Plămănescu**, A. -M. Dumitrescu and M. M. Albu, "High Reporting Rate Smart Metering Data for Enhanced Grid Monitoring and Services for Energy Communities," in IEEE Transactions on Industrial Informatics, vol. 18, no. 6, pp. 4039-4048, June 2022.

[109]. M. Stewart et al., "Integrated multi-scale data analytics and machine learning for the distribution grid," 2017 IEEE International Conference on Smart Grid Communications (SmartGridComm), Dresden, 2017, pp. 423-429.

[110]. M. V. Chilukuri and P. K. Dash, "Multiresolution S-transform-based fuzzy recognition system for power quality events," IEEE Trans. Power Syst., vol. 19, no. 1, pp. 323–330, Feb. 2004.

[111]. Mahmud, et. al., 'The Impact of Prediction Errors in the Domestic Peak Power Demand Management', IEEE Transactions on Industrial Informatics, vol. 16, no. 7, pp. 4567–4579, Jul. 2020.

[112]. Markos Asprou, Ana-Maria Dumitrescu, Elias Kyriakides, Mihaela Albu, 2016, The Impact of PMU Measurement Delays and a Heterogenous Communication Network on a Linear State Estimator, Proc. of the 18th Mediterranean Electrotechnical Conference – MELECON 2016, Limassol, 18-20 April 2016

[113]. N. E. Huang, Z. Shen and S. R. Long, "A new view of nonlinear water waves: The Hilbert spectrum," Annu. Rev. Fluid Mech, vol. 31, p. 417–457, 1999.

[114]. N. E. Huang, Z. Shen, S. R. Long, M. C.Wu, H. H. Shih, Q. Zheng, N. C. Yen, C. C. Tung, and H. H. Liu, "The empirical mode decomposition and the Hilbert spectrum for nonlinear and non-stationary time series analysis," Proc. R. Soc. Lond. A, vol. 454, pp. 903–995, 1998.

[115]. N. Senroy, S. Suryanarayanan and P. F. Ribeiro, "An Improved Hilbert–Huang Method for Analysis of Time-Varying Waveforms in Power Quality," in IEEE Transactions on Power Systems, vol. 22, no. 4, pp. 1843-1850, Nov. 2007.

[116]. N. Uribe-Pérez, L. Hernández, et al., 'State of the Art and Trends Review of Smart Metering in Electricity Grids', Applied Sciences, vol. 6, no. 3, Art. no. 3, Mar. 2016.

[117]. Nechifor, Mihaela Albu, R. Hair, V. Terzija, 2015, A flexible platform for synchronized measurements, data aggregation and information retrieval, Electric Power Systems Research, Elsevier, Vol. 120, March 2015, Page(s): 20-31.

[118]. Network Code on Requirements for Grid Connection Applicable to all Generators, ENTSO-E, Brussels, Belgium, NC RfG/2016, Jul. 2016

[119]. NOBEL GRID project, "D3.4 smart meters architecture and data model analysis v2," 2017. [Online]. Available: https://ec.europa.eu/research/participants/documents/downloadPublic?documentIds=080166e5af5403d3&appId=PPGMS

[120]. NOBEL GRID Project, "D4.1 specification of the unbundled smart meter concept based on commercially existing smart meters," 2015. [Online]. Available: https://ec.europa.eu/research/participants/documents/downloadPublic?documentIds=080166e5a5d135e9&appId=PPGMS

[121]. NREL, Inertia and the Power Grid: A Guide Without the Spin, May 2020.

[122]. Oppenheim, R. Schafer, and J. Buck, Discrete-Time Signal Processing, 2nd ed. Englewood Cliffs, NJ: Prentice-Hall, 1999.

[123]. ORDIN nr. 69 din 15.04.2020, ANRE - Romanian National Regulatory Authority

[124]. P. Kundur, J. Paserba, V. Ajjarapu, G. Andersson, A. Bose, C. Canizares, N. Hatziargyriou, D. Hill, A. Stankovic, C. Taylor, T. Cutsem and V. Vittal, "Definition and classification of power system stability," IEEE Trans. Power Systems, vol. 19, pp. 1387-1401, May 2004.

[125]. P. Li, L. Fei, J. Qian, J. Chen and X. Li, "Based on the improved HHT and its application in the power quality detection of microgrid," in 2011 International Conference on Electrical Machines and Systems, Beijing, 2011.

[126]. P. Li, L. Fei, P. Xi, J. Jie and J. Zhang, "HHT based on the LS-SVM and its application in the voltage flicker and harmonic detection of microgrid," in 2011 4th International Conference on Electric Utility Deregulation and Restructuring and Power Technologies (DRPT), Weihai, Shandong, 2011.

[127]. P. Li, W. Li, C. Liu, X. Xiao and C. Guo, "The new method of harmonic detection in microgrid electric vehicle charging stations based on the improved HHT," in 2012 IEEE International Conference on Power System Technology (POWERCON), Auckland, 2012.

[128]. Pepermans, G., Driesen, J., Haeseldonckx, D. et al. (2005) Distributed generation: definition, benefits and issues. Int. J. Energy Policy, 33 (6), 787–798.

[129]. PeScas Lopes, J.A., Hatziargyriou, N., Mutale, J. et al. (2007) Integrated distributed generation into electric power systems: A review of drivers, challenges and opportunities. Elsevier Electr. Pow. Syst. Res., 77 (9).

[130]. **Plamanescu, R.**, Dumitrescu, A.-M., Albu, M., Suryanarayanan, S. Monitoring LV Prosumers Operation Using Hil-bert—Huang Method. In Proceedings of the 2020 55th International Universities Power Engineering Conference (UPEC), Torino, Italy, 1–4 September 2020, pp. 1–6.

[131]. **Plamanescu, R.**; Dumitrescu, A.-M.; Albu, M.; Suryanarayanan, S. A Hybrid Hilbert-Huang Method for Monitoring Distorted Time-Varying Waveforms. Energies 2021

[132]. Planas, A. Gil-de-Muro, J. Andreu, I. Kortabarria, and I. Martínez de Alegría, "General aspects, hierarchical controls and droop methods in microgrids: A review," Renewable and Sustainable Energy Reviews, vol. 17, pp. 147-159, Jan. 2013.

[133]. R. Deng, Z. Yang, et al., 'A Survey on Demand Response in Smart Grids: Mathematical Models and Approaches', IEEE Transactions on Industrial Informatics, vol. 11, no. 3, pp. 570–582, Jun. 2015.

[134]. R. Godina, E. M. G. Rodrigues, et al., 'Effect of Loads and Other Key Factors on Oil-Transformer Ageing: Sustainability Benefits and Challenges', Energies, vol. 8, no. 10, Oct. 2019.

[135]. R. Messina, V. Vittal, D. Ruiz-Vega and G. Enriquez-Harper, "Interpretation and visualization of wide area PMU measurements using Hilbert analysis," IEEE Trans. Power Systems, vol. 21, no. 4, p. 1760–1771, 2006.

[136]. R. Tomasi et al., "Fostering innovation cooperative energy storage systems: The Storage4Grid project," 2017 IEEE International Conference on Environment and Electrical Engineering and 2017 IEEE Industrial and Commercial Power Systems Europe (EEEIC / I&CPS Europe), 2017, pp. 1-6.

[137]. Rachel Golden and Bentham Paulos – Curtailment of Renewable Energy in California and Beyond, The Electricity Journal, 2015, {https://www.sciencedirect.com/science/article/pii/S1040619015001372

[138]. Raphaël Rinaldi, Ilaria Losa, Michel De Nigris, Ricardo Prata, Mihaela Albu, et al., 2019, ETIP-SNET Vision 2050 – Integrating Smart Networks For The Energy Transition, CIRED 2019 - Open Access Proceedings Journal, vol. 2019, paper 175.

[139]. Raspberry Pi 3 Model B, de tip computer single-board având placa de rețea si conectivitate bluetooth. [Online] disponibil https://www.raspberrypi.com/products/raspberry-pi-3-model-b/

[140]. Riaz, Shariq and Marzooghi, Hesamoddin and Verbič, Gregor and Chapman, Archie C. and Hill, David J. – Generic Demand Model Considering the Impact of Prosumers for Future Grid Scenario Analysis, IEEE Transactions on Smart Grid, 2019.

[141]. Rick Kuffel and Paul Forsyth and Cyprian Peters, The Role and Importance of Real Time Digital Simulation in the Development and Testing of Power System Control and Protection Equipment, IFAC-PapersOnLine, IFAC Workshop on Control of Transmission and Distribution Smart Grids CTDSG 2016.

[142]. Rilling, G., Flandrin, P.; Goncalves, P. On empirical decomposition and its algorithms. In Proceedings of the IEEE-EURASIP Workshop on Nonlinear Signal Image Process, Grado, Italy, 1 January 2003.

[143]. Ruiz-Cortés, Mercedes and González-Romera, Eva and Amaral-Lopes, Rui and Romero-Cadaval, Enrique and Martins, João and Milanés-Montero, María Isabel and Barrero-González, Fermín – Optimal Charge/Discharge Scheduling of Batteries in Microgrids of Prosumers, IEEE Transactions on Energy Conversion, 2019.

[144]. Ruiz-Cortés, Mercedes and González-Romera, Eva and Amaral-Lopes, Rui and Romero-Cadaval, Enrique and Martins, João and Milanés-Montero, María Isabel and Barrero-González, Fermín – Optimal Charge/Discharge Scheduling of Batteries in Microgrids of Prosumers, IEEE Transactions on Energy Conversion, 2019.

[145]. S. Santoso, E. J. Powers, W. M. Grady, and P. Hofmann, "Power quality assessment via wavelet transform," IEEE Trans. Power Del., vol. 11, no. 2, pp. 924–930, Apr. 1996.

[146]. S.I. Vagropoulos, A.G. Bakirtzis, "Optimal bidding strategy for electric vehicle aggregators in electricity markets", IEEE Trans. Power Syst. 28 (2013) 4031–4041.

[147]. Sanduleac, G. Lipari, et al, 'Next Generation Real-Time Smart Meters for ICT Based Assessment of Grid Data Inconsistencies', Energies, vol. 10(7), pp. 857-, June. 2017.

[148]. Sanduleac, Mihai and Albu, Mihaela and Toma, Lucian and Martins, João and Pronto, Anabela Gonçalves and Delgado-Gomes, Vasco – Hybrid AC and DC smart home resilient architecture Transforming prosumers in UniRCons, 2017 International Conference on Engineering, Technology and Innovation (ICE/ITMC).

[149]. Santoso, S.; Powers, E.J.; Grady, W.M.; Hofmann, P. Power quality assessment via wavelet transform analysis. IEEE Trans. Power Deliv. 1996, 11, 924–930.

[150]. Seneviratne C, Ozansoy C. Frequency response due to a large generator loss with the increasing penetration of wind/PV generation - a literature review. Renew Sustain Energy Rev 2016.

[151]. Senroy, N., Suryanarayanan, S., Ribeiro, P.F. An Improved Hilbert–Huang Method for Analysis of Time-Varying Waveforms in Power Quality. IEEE Trans.Power Syst. 2007, 22, 1843–1850.

[152]. Shengqing, L., Huanyue, Z., Wenxiang, X., Weizhou, L. A Harmonic Current Forecasting Method for Microgrid HAPF Based on the EMD-SVR Theory. In Proceedings of the 2013 Third International Conference on Intelligent System Design and En-gineering Applications, Hong Kong, 16–18 January 2013.

[153]. Sidorov et al., 'A Dynamic Analysis of Energy Storage With Renewable and Diesel Generation Using Volterra Equations', IEEE Trans. on Industrial Informatics, vol. 16, pp. 3451–3459, May 2020.

[154]. Soni N, Doolla S, Chandorkar MC. Improvement of transient response in microgrids using virtual inertia. IEEE Trans Power Deliv 2013.

[155]. Stockwell, R.G.; Mansinha, L.; Lowe, R.P. Localization of the complex spectrum: the S transform. IEEE Trans. Signal Process. 1996, 44, 998–1001.

[156]. T. Logenthiran, et.al., "Multiagent system for real-time operation of a microgrid in real-time digital simulator," IEEE Trans. on Smart Grid, vol. 3, no. 2, pp. 925-933, 2012.

[157]. Terzija, G. Valverde, D. Cai, P. Regulski, V. Madani, J. Fitch, S. Skok, M. M Begovic, A. Phadke, "Wide-area monitoring, protection, and control of future electric power networks", Proc.of the IEEE, Vol. 99(1), 2011, pp. 80-93.

[158]. Testa, A.; Gallo, D.; Langella, R. On the Processing of Harmonics and Interharmonics: Using Hanning Window in Standard Framework. IEEE Trans. Power Deliv. 2004, 19, 28–34.

[159]. Tielens P, Van Hertem D, Hertem D Van. The relevance of inertia in power systems. Renew Sustain Energy Rev 2016;55:999–1009.

[160]. TyphoonHIL, About Real-time simulation in Typhoon HIL, url = "https://www.typhoon-hil.com", accessed: 01.09.2021

[161]. W. Galli, G. T. Heydt, and P. F. Ribeiro, "Exploring the power of wavelet analysis," IEEE Comput. Appl. Power, vol. 9, no. 4, pp. 37–41, Oct. 1996.

[162]. W. Luan, J. Peng, et. al,, "Smart Meter Data Analytics for Distribution Network Connectivity Verification," in IEEE Trans. on Smart Grid, vol. 6, no. 4, pp. 1964-1971, July 2015.

[163]. Wang, Q. Chen, et al., 'Review of Smart Meter Data Analytics: Applications, Methodologies, and Challenges', IEEE Transactions on Smart Grid, vol. 10, no. 3, pp. 3125–3148, May 2019.

[164]. Working Group C6, CIGRE – Active distribution systems and distributed energy resources – technical brochure, "hybrid systems for off-grid power supply Reference 826, March 2021

[165]. Y. Wang, X. Zeng and J. Hu, "HHT energy spectrum based identification method for lightning fault," in 2011 International Conference on Advanced Power System Automation and Protection, Beijing, 2011.

[166]. Y. Yang, W. Li, et al., 'Bayesian Deep Learning-Based Probabilistic Load Forecasting in Smart Grids', IEEE Transactions on Industrial Informatics, vol. 16, no. 7, pp. 4703–4713, Jul. 2020.

[167]. Y. Zhu, et al. "Matrix Profile XI: SCRIMP++: Time Series Motif Discovery at Interactive Speeds," ICDM 2018

[168]. Yuan, Yuxuan, Wang, Zhaoyu – Mining Smart Meter Data to Enhance Distribution Grid Observability for Behind-the-Meter Load Control: Significantly improving system situational awareness and providing valuable insights, IEEE Electrification Magazine, 2021.

[169]. Zhang, Y.; Su, N.; Li, Z.; Gou, Z.; Chen, Q.; Zhang, Y. Assessment of arterial distension based on continuous wave Doppler ultrasound with an improved Hilbert-Huang processing. IEEE Trans. Ultrason. Ferroelectr. Freq. Control. 2009, 57, 203–213.